Performance of bias correction schemes for CMORPH rainfall estimates in the Zambezi River Basin

Webster Gumindoga[12], Tom. H.M. Rientjes[1], Alemseged.T. Haile[3], Hodson Makurira[2] and Paolo Reggiani[4]

[1]Faculty ITC, University of Twente, The Netherlands
[2]Civil Engineering Department, University of Zimbabwe, Zimbabwe
[3]International Water Management Institute (IWMI), Ethiopia
[4]University of Siegen, Germany

Email of corresponding author: w.gumindoga@utwente.nl

Submission: 29 October 2018

Email of corresponding author: w.gumindoga@utwente.nl

Abstract

Satellite Rainfall Estimates (SRE) are prone to bias as they are indirect derivatives of the visible, infrared, and/or microwave cloud properties, hence SREs need correction. We evaluate the influence of elevation and distance from large scale open water bodies on bias for Climate Prediction Center-MORPHing (CMORPH) rainfall estimates in the Zambezi Basin. The effectiveness of five linear/non-linear and time-space variant/invariant bias correction schemes was evaluated for daily rainfall estimates and climatic seasonality. Schemes used are: Spatio-temporal Bias (STB), Elevation zone bias (EZ), Power transform (PT), Distribution transformation (DT) and the Quantile mapping based on an empirical distribution (QME). We used daily time series (1998-2013) from 60 gauge stations and CMORPH SREs for the Zambezi Basin. To evaluate effectiveness of the bias correction techniques, spatial and temporal cross-validation was applied based on 8 stations and on the 1998-1999 CMORPH time series, respectively. For correction, STB and EZ schemes proved to be more effective in removing bias. STB improved the correlation coefficient and Nash Sutcliffe efficiency by 50 % and 53 % respectively and reduced the root mean squared difference and relative bias by 25 % and 33 % respectively. Paired t-tests showed that there is no significant difference ($p < 0.05$) in the daily means of CMORPH against gauge rainfall after bias correction. ANOVA post-hoc tests revealed that the STB and EZ bias correction schemes are preferable. Bias is highest for the very light rainfall (<2.5 mm/d), for which most effective bias reduction is shown, in particular for the wet season. Similar findings are shown through quantile-quantile (q-q) plots. The spatial cross-validation approach revealed that the majority of the bias correction schemes removed bias by > 28 %. The temporal cross-validation approach showed effectiveness of the bias correction schemes. Taylor diagrams show that station elevation has an influence on CMORPH performance. Effects of distance >10m from large scale open water bodies are minimum whereas the effect at shorter distances are indicated but not conclusive by lack of rain gauges. Findings of this study show the importance of applying bias correction to SREs.

Keywords: *distance zone, elevation zone, satellite rainfall estimates, spatio-temporal bias, Taylor diagram*

1. Introduction

Correction schemes for rainfall estimates are developed for climate models (Maraun, 2016;Grillakis et al., 2017;Switanek et al., 2017), for radar approaches (Cecinati et al., 2017;Yoo et al., 2014) and for satellite based, multi-sensor approaches (Najmaddin et al., 2017;Valdés-Pineda et al., 2016). In this study focus is on satellite rainfall estimates (SREs) to improve reliability in spatio-temporal rainfall representation.

Studies in satellite based rainfall estimation show that estimates are prone to systematic and random errors (Gebregiorgis et al., 2012;Habib et al., 2014;Shrestha, 2011;Tesfagiorgis et al., 2011;Vernimmen et al., 2012;Woody et al., 2014). Errors result primarily from the indirect estimation of rainfall from visible (VIS), infrared (IR), and/or microwave (MW) based satellite remote sensing of cloud properties (Pereira Filho et al., 2010; Romano et al., 2017). Systematic errors in SREs commonly are referred to as bias, which is a measure that indicates the accumulated difference between rain gauge observations and SREs. Bias in SREs is expressed for rainfall depth (Habib et al., 2012b), rain rate (Haile et al., 2013) and frequency at which rain rates occur (Khan et al., 2014). Bias may be negative or positive where negative bias indicates underestimation whereas positive bias indicates overestimation (Liu, 2015; Moazami et al., 2013).

Recent studies on the National Oceanic and Atmospheric Administration (NOAA) Climate Prediction Center-MORPHing (CMORPH) (Wehbe et al., 2017;Jiang et al., 2016; Liu et al., 2015; Haile et al., 2015) reveal that accuracy of this satellite rainfall product varies across different regions, but causes are not directly indentifiable. As such correction schemes serve to reduce systematic errors and to improve applicability of SREs. Correction schemes rely on assumptions that adjust errors in space and/or time (Habib et al., 2014). Some correction schemes consider correction only for spatial distributed patterns in bias, commonly known as space variant/invariant. Approaches that correct for spatially averaged bias have roots in radar rainfall estimation (Seo et al., 1999) but are unsuitable for large scale basins (> 5,000 km^2) where rainfall may substantially vary in space (Habib et al., 2014). Studies by Tefsagiorgis et al. (2011) in Oklahoma (USA) and Müller and Thompson (2013) in Nepal concluded that space variant correction schemes are more effective in reducing CMORPH and TRMM bias than space invariant correction schemes. In a study conducted in the Upper Blue Nile basin in Ethiopia, Bhatti et al. (2016) show that CMORPH bias correction is most effective when bias factors are calculated for 7 day sequential windows.

Bias correction schemes based on regression techniques have reported distortion of frequency of rainfall rates (Ines and Hansen, 2006;Marcos et al., 2018). Multiplicative shift procedures tend to adjust SRE rainfall rates, but Ines and Hansen (2006) reported that they do not correct systematic errors in rainfall frequency of climate models. Non-multiplicative bias correction schemes preserve the timing of rainfall within a season (Fang et al., 2015;Hempel et al., 2013). Studies that have applied non-linear bias correction schemes such as Power Function report correction of extreme values (depth, rate and frequency) thus mitigating the underestimation and overestimation of CMORPH rainfall (Vernimmen et al., 2012). The study by Tian (2010) in the United States noted that the Bayesian (likelihood) analysis techniques are found to over-adjust both light and heavy CMORPH rainfall.

Bias often exhibits a topographic and latitudinal dependency as, for instance, shown for CMORPH product in the Nile Basin (Bitew et al., 2011; Habib et al., 2012a; Haile et al., 2013). For Southern Africa, Thorne et al. (2001), Dinku et al. (2008) and Meyer et al. (2017) show that bias in rainfall rate and frequency can be related to location, topography, local climate and season. First studies in the Zambezi Basin (Southern Africa) on SREs show evidence that necessitates correction of SREs. For example, Cohen Liechti (2012) show bias in CMORPH SREs for daily rainfall and for accumulated rainfall at monthly scale. Matos et al. (2013), Thiemig et al. (2012) and Toté et al. (2015) show that bias in rainfall depth at time intervals ranging from daily to monthly varies across geographical domains in the Zambezi Basin and may be as large as ±50 %. Besides elevation, there are indications that presence of Lake Tana (≈ 3050 km^2, Ethiopia) affects rainfall at short distances (<10km) (Haile et al., 2009; Rientjes et al., 2013a).

For less developed areas such as in the Zambezi Basin that is selected for this study, studies on SREs are limited. This is despite the strategic importance of the basin in providing water to over 30 million people (World Bank, 2010a). An exception is the study by Beyer et al. (2014) on correction of the TRMM-3B42 product for agricultural purposes in the Upper Zambezi Basin. Studies (Cohen Liechti et al., 2012; Meier et al., 2011) on use of SREs in the Zambezi

River Basin mainly focused on accuracy assessment of the SREs using standard statistical indicators with little or no effort to perform bias correction despite the evidence of errors in these products. The use of uncorrected SREs is reported for hydrological modelling in the Nile Basin (Bitew and Gebremichael, 2011) and Zambezi Basin (Cohen Liechti et al., 2012), respectively, and for drought monitoring in Mozambique (Toté et al., 2015). The poor performance of SREs in above studies urges for bias correction to result in more accurate rainfall representation. The selection of CMORPH satellite rainfall for this study is based on successful applications of bias corrected CMORPH estimates in African basins for hydrological modelling (Habib et al., 2014) and flood predictions in West Africa (Thiemig et al., 2013). In first publications on CMORPH, Joyce et al. (2004) describe CMORPH as a gridded precipitation product that estimates rainfall with information derived from IR data and MW data. CMORPH combines the retrieval accuracy of passive MW estimates with IR measurements which are available at high temporal resolution but with low accuracy. The important distinction between CMORPH and other merging methods is that the IR data are not used for rainfall estimation but used only to propagate rainfall features that have been derived from microwave data. The flexible 'morphing' technique is applied to modify the shape and rate of rainfall patterns. CMORPH is operational since 2002 for which data is available at the CPC of the National Centers for Environmental Prediction (NCEP) (after http://www.ncep.noaa.gov/). Recent publications on CMORPH in African basins exist (Wehbe et al., 2017;Koutsouris et al., 2016;Jiang et al., 2016;Haile et al., 2015). However, studies on bias correction of CMORPH in the semi-arid Zambezi Basin are limited.

In this study we use daily CMORPH and rain gauge data for Upper, Middle, and Lower Zambezi basins to (1) evaluate if performance of CMORPH rainfall is affected by elevation and distance from large scale open water bodies (2) evaluate the effectiveness of linear/non-linear and time-space variant/invariant bias correction schemes and (3) assess the performance of bias correction schemes to represent different rainfall rates and climate seasonality. Analysis serve to improve reliability of SREs applications in water resource applications in the Zambezi basin such as for rainfall-runoff modeling

2. Study area

The Zambezi River is the fourth-longest river (~2,574 km) in Africa with basin area of ~1,390,000 km^2 (~4 % of the African continent). The river drains into the Indian Ocean and has mean annual discharge of 4,134 m^3/s (World Bank, 2010a). The river has its source in Zambia with basin boundaries in Angola, Namibia Botswana, Zambia, Zimbabwe and Mozambique (Fig. 1). The basin is characterized by considerable differences in elevation and topography, distinct climatic seasons and presence of large scale open water bodies and, as such, makes the basin well suited for this study. The basin is divided into three sub-basins i.e., the Lower Zambezi comprising the Tete, Lake Malawi/Shire, and Zambezi Delta basins, the Middle Zambezi comprising the Kariba, Mupata, Kafue, and Luangwa basins, and the Upper Zambezi comprising the Kabompo, Lungwebungo, Luanginga, Barotse, and Cuando/Chobe basins (Beilfuss, 2012).

The elevation of the Zambezi basin ranges from < 200 m (for some parts of Mozambique) to >1500 m above sea level (for some parts of Zambia). Large scale open water bodies in and around the basin are Kariba, Cabora Bassa, Bangweulu, Chilwa and Nyasa. The Indian Ocean lies to the east of Mozambique. Typical landcover types are woodland, grassland, water surfaces and cropland (Beilfuss et al., 2000). The basin lies in the tropics between 10 and 20 degrees South, encompassing humid, semi-arid and arid regions dominated by seasonal rainfall patterns associated with the Inter-Tropical Convergence Zone (ITCZ), a convective front oscillating along the equator (Cohen Liechti et al., 2012). The movement of the ITCZ in Southern hemisphere results in the peak rainy season that occurs during the summer (October to April) and the dry winter months (May-Sept) is a result of the shifting back of ITCZ towards the equator (Schlosser and Strzepek, 2015). The weather system in South Eastern parts such as Mozambique is dominated by Antarctic Polar Fronts (APF) and Tropical Temperate Troughs (TTTs) occurrence which is positively related to La Niña and Southern Hemisphere planetary waves, while El Niño-Southern Oscillation (ENSO) appears to play a significant role in causing dry conditions in the basin (Beilfuss, 2012).

The basin is characterized by high annual rainfall (>1,400 mm/yr) in the northern and north-eastern areas and by low annual rainfall (<500 mm/yr) in the southern and western parts (World Bank, 2010b). Due to this rainfall distribution, northern tributaries in the Upper Zambezi sub-basin contribute 60 % of the mean annual discharge (Tumbare, 2000). The river and its tributaries are subject to seasonal floods and droughts that have devastating effects on the people and economies of the region, especially the poorest members of the population

(Tumbare, 2005). It is not uncommon to experience both floods and droughts within the same hydrological year.

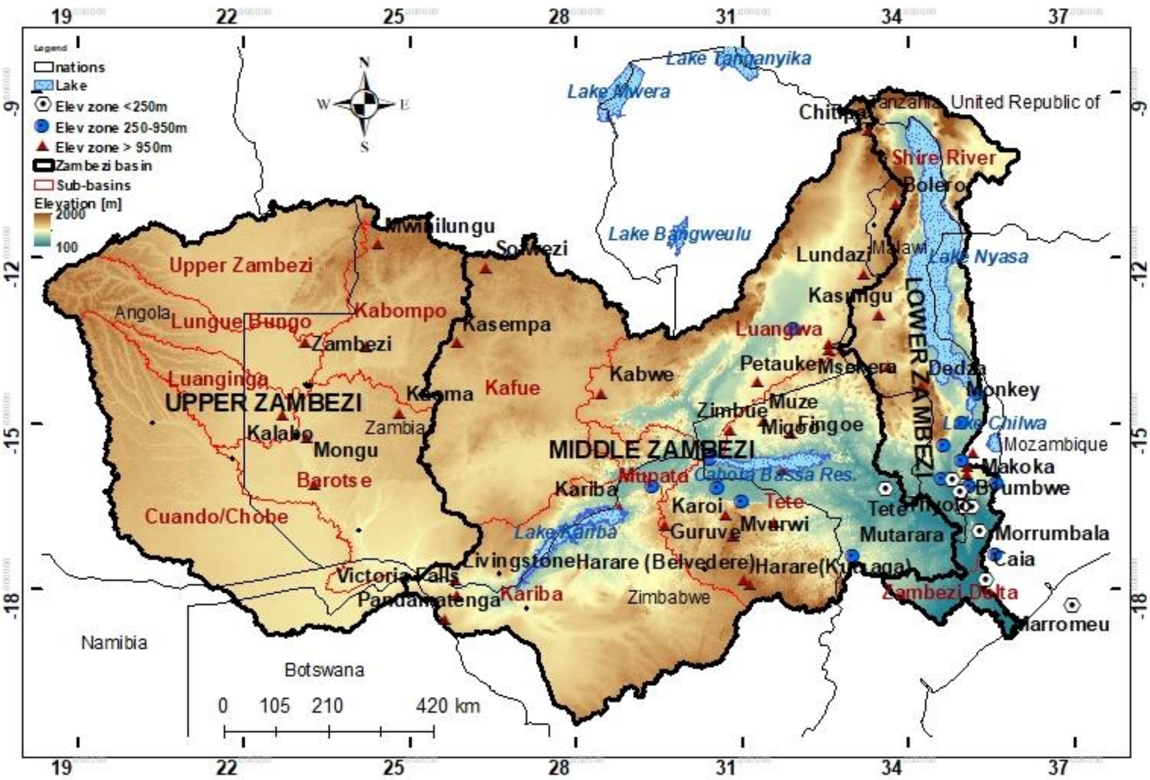

Figure 1: Zambezi River Basin from Africa with sub basins, major lakes, elevation, and locations and names of the 60 rain gauging stations (in each respective elevation zone) used in this study.

3. Materials and Methodology

3.1. Rainfall data

3.1.1. CMORPH

For this study, time series of CMORPH rainfall images (1998-2013) at 8 km × 8 km, 30-minute resolution were selected and downloaded from the NOAA repository (ftp://ftp.cpc.ncep.noaa.gov/prep/CMORPH_V1.0/CRT/8km.30m/). Images are downloaded by means of the GeoNETCAST ISOD toolbox of ILWIS GIS software (http://52north.org/downloads/). Half hourly estimates were aggregated to daily totals to match the observation interval of gauge based daily rainfall.

3.1.2. Rain gauge network

Time series of daily rainfall from 60 stations were obtained from meteorological departments in Botswana, Malawi, Mozambique, Zambia and Zimbabwe for stations that cover the study area. All the stations are standard type rain gauges with a measuring cylinder whose unit of measurement is millimetres (mm).

Some stations are affected by data gaps but the available time series are of sufficiently long duration (see Appendix 1) to serve the objectives of this study. Stations are irregularly distributed across the vast basin and are located at elevation between 3 m to 1575 m (Figure 1). The minimum, maximum and average distance between the rain gauges is 3.5 km (Zumbo in Mozambique-Kanyemba in Zimbabwe), 1570 km (Mwinilunga in Zambia-Marromeu in Mozambique) and 565 km respectively. Distances to large scale open water bodies range between 5 km and 615 km. This allows us to evaluate if elevation and distance to large scale open water bodies affect CMORPH performance.

3.1.3. Comparison of CMORPH and gauge rainfall

In this study, we compare gauge rainfall at point scale to CMORPH satellite derived rainfall estimates at pixel scale (point-to-pixel). Comparison is at a daily time interval covering the period 1998-2013, following Cohen Liechti et al. (2012), Dinku et al. (2008), Haile et al. (2014), Hughes (2006), Tsidu (2012) and Worqlul et al. (2014) who report on point-to-pixel comparisons in African basins. We apply point-to-pixel comparison to rule out any aspect of interpolation error as a consequence of the low density network with unevenly distributed stations. We refer to Heidinger et al. (2012), Li and Heap (2011), Tobin and Bennett (2010) and Yin et al. (2008) who report that interpolation introduces unreliability and uncertainty to pixel based rainfall estimates. Also, Worqlul et al. (2014) describe that for pixel-to-pixel comparison, there is demand for a well distributed rain gauge network that would not hamper accurate interpolation.

3.2. Elevation and distance from large scale open water bodies

Habib et al. (2012a), Haile et al. (2009) and Rientjes et al. (2013a) for the Nile Basin reveal that elevation affect performance of SREs. Findings in the latter two studies signal that performance possibly also may be affected by presence of Lake Tana. To assess both influences, we classified the Zambezi Basin into 3 elevation zones for which the hierarchical cluster ‘within-groups linkage’ method in the Statistical Product and Service Solutions (SPSS) software was used (Table 1). Based on Euclidian distance to large-scale open water bodies, 4 arbitrary distance zones are defined to group stations (Table 1). A detailed description on the individual stations, their elevation and distance to large-scale open water bodies is provided in Appendix 1. The Advanced Spaceborne Thermal Emission and Reflection Radiometer (ASTER) based DEM of 30 m resolution obtained from http://gdem.ersdac.jspacesystems.or.jp/, is used to represent elevation across the Zambezi Basin. The Euclidian distance of each rain gauge location to large-scale open water bodies is defined in a GIS environment through the distance calculation algorithm. Large-scale open water bodies are defined as perennial open water bodies with surface area > 700 km^2. The threshold is defined based on knowledge of the water bodies in the study area. A preliminary analysis on 300 water bodies in the study area revealed that only surface areas > 700 km^2 induce notable effect on rainfall patterns.

Table 1: Elevation and distance from large scale open water bodies

Zone ID	Elevation (m)	No. of stations	Mean elevation of stations (m)
Zone 1	< 250	8	90
Zone 2	250-950	21	510
Zone 3	> 950	31	1140
Zone ID	Distance (km)	No. of stations	Mean distance to large-scale open water bodies (km)
Zone 1	< 10 km	4	5
Zone 2	10 - 50	10	35
Zone 3	50 - 100	18	80
Zone 4	> 100	28	275

3.3. Bias correction schemes

Bias correction schemes evaluated in this study are the Spatio-temporal bias (STB), Elevation zone bias (EZ), Power transform (PT), Distribution transformation (DT), and the Quantile mapping based on an empirical distribution (QME), this by our aim to correct for bias while daily rainfall variability is preserved. The five schemes are chosen based on merits documented in literature (Bhatti et al., 2016; Habib et al., 2014; Teutschbein and Seibert, 2013; Themeßl et al., 2012; Vernimmen et al., 2012). We note that findings on the performance of selected bias correction schemes in literature do not allow for generalization but findings only apply to the respective study domains (Wehbe et al., 2017;Jiang et al., 2016;Liu et al., 2015;Haile et al., 2015).

In the procedure to define a time window for bias correction we follow Habib et al. (2014) and Bhatti et al. (2016) who in the Lake Tana Basin (Ethiopia) carried out a sensitivity analysis on moving time windows and on sequential time windows. Window lengths of 3 and 31 days are tested. Findings indicated that a 7-day sequential time window for bias factors is most appropriate but only when a minimum of five rainy days were recorded within the 7-day window with a minimum rainfall accumulation depth of 5 mm, otherwise no bias is estimated (i.e. a value of 1 applies as bias correction factor). Preliminary tests in this study on 5 and 7-day moving and sequential windows on 20 individual stations distributed over the three elevation zones indicates that the 7-day sequential approach is well applicable in the Zambezi Basin. As such, the approach was selected.

The bias correction factors are calculated using only rain days (rainfall ≥ 1 mm). Otherwise in cases where both the gauge and satellite have zero values (RG=0 and CMORPH =0), correction is not applied and the SRE value remains 0 mm/day.

Following Bhatti et al. (2016), we spatially interpolate the bias correction factors of the rain gauges so that SREs at all pixels can be corrected. For interpolation, the Universal Kriging was applied. Thus to systematically correct all CMORPH estimates, station based bias factors for each time window are spatially interpolated to arrive at spatial coverage across the study area and to allow for comparison with other approaches.

3.3.1. Spatio-temporal bias correction (STB)

This linear bias correction scheme has its origin in the correction of radar based precipitation estimates (Tesfagiorgis et al., 2011) and downscaled precipitation products from climate models. The CMORPH daily rainfall estimates (S) are multiplied by the bias correction factor for the respective sequential time window for individual stations resulting in corrected CMORPH estimates (STB) in a temporally and spatially coherent manner (Equation [1]).

$$STB = S \frac{\sum_{t=d}^{t=d-l} G(i,t)}{\sum_{t=d}^{t=d-l} S(i,t)} \quad \textbf{[1]}$$

Where:

G = gauged rainfall (mm/day)

i = gauge number

d = day number

t = julian day number

l = length of a time window for bias correction

The advantages of this bias correction scheme is that it is straightforward and easy to implement due to its simplicity and modest data requirements. However, just like any multiplicative shift procedures of bias correction, STB has challenges in correct systematic errors in rainfall frequency particularly the wet-day frequencies (Lenderink et al., 2007; Teutschbein and Seibert, 2013).

3.3.2. Elevation zone bias correction (EZ)

This bias scheme is proposed in this study and aims at correcting satellite rainfall for elevation influences. This method groups rain gauge stations into 3 elevation zones based on station elevation. The grouping in this study is based on the hierarchical clustering technique, expert knowledge about the study area but also guided by relevant past studies in the basin (e.g. World Bank, 2010b;Beilfuss, 2012). Each zone has the same bias correction factor but differs across the three zones. In the time domain bias factors vary following the 7-day sequential window approach. The corrected CMORPH estimates (EZ) at daily time interval are obtained by multiplying the uncorrected CMORPH daily rainfall estimates (*S*) by the daily bias correction factor of each elevation zone.

$$EZ = S\,\frac{\sum_{t=d}^{t=d-l}\sum_{i=1}^{i=n} G(i,t)}{\sum_{t=d}^{t=d-l}\sum_{i=1}^{i=n} S(i,t)} \qquad \textbf{[2]}$$

The merits of this bias correction scheme is that the effects of elevation on rainfall depth are accounted for. SREs often have difficulties in capturing rainfall events due to orographic effects and thus require elevation based correction.

3.3.3. Power transform (PT)

The non-linear PT bias correction scheme has its origin in studies of climate change impact (Lafon et al., 2013). Vernimmen et al. (2012) show that the scheme could be applied to correct satellite rainfall estimates for use in hydrological modelling and drought monitoring. The PT method uses an exponential form to adjust the standard deviation of rainfall series. The daily bias corrected CMORPH rainfall (PT) for a pixel that overlays a station is obtained using equation:

$$PT = aG(i,t)^{b} \qquad \textbf{[3]}$$

Where:

G = gauged rainfall (mm/day)

a = prefactor such that the mean of the transformed CMORPH values is equal to the mean of rain gauge rainfall

b = factor calculated such that for each rain gauge the coefficient of variation (CV) of CMORPH matches the gauge based counter parts

i = gauge number

t = day number

Optimized values for a and b are obtained through the generalized reduced gradient algorithm (Fylstra et al., 1998). Values for a and b vary for the 7-day time sequential window since correction is at daily time base. In the case of utilizing the PT method in a certain area (or for a certain period), the bias correction factor is spatially interpolated to result in comparable estimates with other bias correction schemes. The advantage of the bias scheme is that it adjusts extreme precipitation values in CMORPH estimates (Vernimmen et al., 2012). PT has reported limitations in correcting wet-day frequencies and intensities (Leander et al., 2008; Teutschbein and Seibert, 2013).

3.3.4. Distribution transformation (DT)

DT is an additive bias correction approach which has its origin in statistical downscaling of climate model data (Bouwer et al., 2004). The method transforms a statistical distribution function of daily CMORPH rainfall estimates to match the distibution by gauged rainfall. The procedure to match the CMORPH distribution function to gauge rainfall based counter parts is described in equations [4-8]. The principle to matching is that the difference in the mean value and differences in the variance are corrected for, in the 7-day sequential window. First, the bias correction factor for the mean (DTu) is determined by equation [4]:

$$DT_u = \frac{G_u}{S_u} \quad \textbf{[4]}$$

G_u and S_u are mean values of 7-day gauge and CMORPH rainfall estimates.

Secondly, the correction factor for the variance ($DT\tau$) is determined by the quotient of the 7-day standard deviations, $G\tau$ and $S\tau$, for gauge and CMORPH respectively.

$$DT\tau = \frac{G\tau}{S\tau} \quad \textbf{[5]}$$

Once the correction factors which vary within a 7-day time sequential window are established, they are then applied to correct all daily CMORPH estimates (S) through equation [6] to obtain corrected CMORPH rainfall estimate (DT). The parameters *DTu* and $DT\tau$ are developed within a 7-day sequential window but correction is at daily time intervals.

$$DT = (S(i,t) - Su)DT\tau \; + DTu * S\tau \quad \textbf{[6]}$$

Uncorrected CMORPH daily values are returned if [6] results in negative values. The merit of this bias correction scheme is that it corrects wet-day frequencies and intensities. The disadvantage of this bias correction scheme is that adding the gauge based mean deviation to the satellite data destroys the physical consistency of the data. In addition, the method might result in the generation of too few rain days in the wet season, and sometimes the mean of daily intensities might be unrealistically corrected (Johnson and Sharma, 2011; Teutschbein and Seibert, 2013).

3.3.5. Quantile mapping based on an empirical distribution (QME)

This is a quantile based empirical-statistical error correction method with its origin in empirical transformation and bias correction of regional climate model-simulated precipitation (Themeßl et al., 2012). The method corrects CMORPH precipitation based on empirical cumulative distribution functions (*ecdfs*) which are established for each 7-day time window and for each station. The bias corrected rainfall (*QME*) using quantile mapping are expressed in terms of the empirical cumulative distribution function (*ecdf*) and its inverse (ecdf^{-1}). Parameters apply to a 7-day sequential window but correction is then at daily time interval with bias spatially averaged for the entire domain to allow for comparison with other approaches

$$QME = ecdf_{obs}^{-1}(ecdf_{raw}(S(i,t))) \quad \textbf{[7]}$$

Where:

$ecdf_{obs}$ = empirical cumulative distribution function for the gauge based observation

$ecdf_{raw}$ = empirical cumulative distribution function for the uncorrected CMORPH

The advantage of this bias scheme is that it corrects quantiles and preserves the extreme precipitation values (Themeßl et al., 2012). However, it also has its limitation due to the assumption that both the observed and satellite rainfall follow the same proposed distribution, which may introduce potential new biases.

3.4. Rainfall rates and seasons

To assess the performance of SREs for different classes of daily rainfall rates five classes are defined which indicate: very light (< 2.5 mm/day), light (2.5-5.0), moderate (5.0-10.0 mm/day), heavy (10.0-20.0 mm/day) and very heavy rainfall (> 20 mm/day).

Furthermore, gauged rainfall was divided into wet and dry seasonal periods to assess the influence of seasonality on performance of bias correction schemes. The wet season in the Zambezi Basin spans from October-March whereas the dry season spans from April-September.

3.5. Evaluation of CMORPH estimates

Corrected and uncorrected CMORPH satellite rainfall estimates are evaluated with reference to rain gauge rainfall using statistics that measure systematic differences (i.e. percentage bias and Mean Absolute Error (MAE)), measures of association (e.g. correlation coefficient and Nash Sutcliffe Efficency (NSE) and random differences (e.g. standard deviation of differences and coefficient of variation) (Haile et al., 2013). Bias is a measure of how the satellite rainfall estimate deviates from the rain gauge rainfall, and the result is normalised by the summation of the gauge values. A positive value indicates overestimation whereas a negative value indicates underestimation. The correlation coefficient (ranging between +1 and −1) represents the linear dependence of gauge and CMORPH data. MAE is the arithmetic average of the absolute values of the differences between the daily gauge and CMORPH satellite rainfall estimates. The MAE is zero if the rainfall estimates are perfect and increases as discrepancies between the gauge and satellite become larger. NSE indicates how well the satellite rainfall matches the rain gauge observation and it ranges between - ∞ and 1, with NSE = 1 meaning a perfect fit (Nash and Sutcliffe, 1970).

Equations [8-11] apply.

$$bias\ (\%) = \frac{\sum(S-G)}{\sum G} * 100 \quad \textbf{[8]}$$

$$R = \frac{\sum(G-\overline{G})(S-\overline{S})}{\sqrt{\sum(G-\overline{G})^2}\sqrt{\sum(S-\overline{S})^2}} \quad \textbf{[9]}$$

$$MAE = \frac{1}{n}\sum |S-G| \quad \textbf{[10]}$$

$$NSE = \frac{\sum(G-S)^2}{\sum(G-\overline{G})^2} \quad \textbf{[11]}$$

Where:

S = satellite rainfall estimates (mm/day)

$\bar{S}$ = mean of the satellite rainfall estimates (mm/day)

G = rainfall by a rain gauge (mm/day)

$\bar{G}$ = mean values of rainfall recorded by a rain gauge (mm/day)

n = number of observations

3.6. Test for differences of mean

To detect significant differences between gauge and satellite rainfall (corrected and uncorrected) and differences amongst the five bias correction methods described in Section 3.3, we apply paired t-test and analysis of variance (ANOVA) tests.

3.6.1. Paired t-tests

A paired t-test was used to test whether there is a significant difference between rain gauge, uncorrected and bias corrected CMORPH satellite rainfall for the 52 rain gauges. Results are summarized for the Upper, Lower and Middle Zambezi. The paired t-test compares the mean difference of the values to zero. It depends on the mean difference, the variability of the differences and the number of data. The null hypothesis (H_0) is that there is no difference in mean gauge and satellite daily rainfall (uncorrected and bias corrected). If the p-value is less than or equal 0.05 (5%), the result is deemed statistically significant, i.e., there is a significant relationship between the gauge and satellite rainfall (Wilks, 2006; Field, 2009).

3.6.2. Analysis of Variance (ANOVA) test

The ANOVA-test aims to test whether there is a significant difference amongst the 5 bias correction techniques. The Null hypothesis (H_0) is that there are no differences amongst the five bias correction schemes. We further determined which schemes differ significantly using 3 post-hoc tests, namely: Tukey HSD, Schefe and the Bonferroni (Brown, 2005; Kucuk et al., 2018). Results are summarized for the Upper, Lower and Middle Zambezi.

3.7. Taylor diagram

We apply a Taylor diagram to evaluate differences in data sets generated by respective bias correction schemes by providing a summary of how well bias correction results match gauge rainfall in terms of pattern, variability and magnitude of the variability. Visual comparison of SRE performance is done by analysing how well patterns match each other in terms of the Pearson's product-moment correlation coefficient (R), root mean square difference (E), and the ratio of variances on a 2-D plot (Lo Conti et al., 2014;Taylor, 2001). The reason that each point in the two-dimensional space of the Taylor diagram can represent the above three different statistics simultaneously is that the centered pattern of root mean square difference (E^i), and the ratio of variances are related by the following:

$$E^i = \sqrt{\sigma_f^2 + \sigma_r^2 - 2\sigma_f \sigma_r R} \qquad \textbf{[12]}$$

Where:

σ_f and σ_r = standard deviation of CMORPH and rain gauge rainfall, respectively.

Development and applications of Taylor diagrams have roots in climate change studies (Smiatek et al., 2016;Taylor, 2001) but also has frequent applications in environmental model evaluation studies (Cuvelier et al., 2007;Dennis et al., 2010;Srivastava et al., 2015). Bhatti et al. (2016) propose the use of Taylor Diagrams for assessing effectiveness of SREs bias correction schemes. The most effective bias correction schemes will have data that lie near a point marked ‘reference’ on the x-axis, relatively high correlation coefficient and low root mean square difference. Bias correction schemes matching gauged based standard deviation have patterns that have the right amplitude.

3.8. Quantile-quantile (q-q) plots

A q-q plot is used to check if two datasets (in this case gauge vs CMORPH rainfall) can fit the same distribution (Wilks, 2006). A q-q plot is a plot of the quantiles of the first data set against the quantiles of the second data set. A 45-degree reference line is also plotted. If the satellite rainfall (corrected and uncorrected) has the same distribution as the rainguage, the points should fall approximately along this reference line. The greater the departure from this reference line, the greater the evidence for the conclusion that the bias correction scheme is less effective (NIST/SEMATECH, 2001).

The main advantage of the q-q plot is that many distributional aspects can be simultaneously tested. For example, changes in symmetry, and the presence of outliers can all be detected from this plot.

3.9. Cross validation of bias correction

3.9.1. Spatial cross-validation

The spatial cross-validation procedure (hold-out sample) applied in this study, involves the withdrawal of 8 in-situ stations from the sample of 60 when generating bias corrected SREs for all pixels across the study area. Corrected SREs are then compared to the rain gauge rainfall of the withdrawn stations to evaluate closeness of match. From the sample of 8 we selected 2 stations in the < 250 m elevation zone, 3 stations in the 250-950 m zone and 3 stations in > 950 m elevation zone. Stations selected have elevation close to the average elevation zone value and are centred in an elevation zone. This left us with 52 stations for applying the bias correction methods and spatial interpolation. As performance indicators to evaluate results of cross-validation, we use the percentage bias, MAE, Correlation Coefficient and the estimated ratio which is obtained by dividing CMORPH rainfall totals and gauge based rainfall totals for the 1999-2013 period.

3.9.2. Temporal cross-validation

For evaluation of SREs in the time domain we followed Gutjahr and Heinemann (2013) to omit rainfall (both from gauge and satellite) for the 1998-1999 hydrological year to remain with 14 years for bias correction of SREs. Bias corrected estimates for the 14 years are then evaluated against estimates for 1998-1999 period that served as reference. For evaluation we use the percentage bias, MAE, correlation coefficient and the estimated ratio, that all are averaged for the Upper, Middle and Lower Zambezi but also for the wet and dry seasons.

4. Results and Discussion

4.1. Performance of uncorrected CMORPH rainfall

The spatially interpolated values of bias (%) accross the Zambezi Basin are shown in Figure 2. Areas in the central and western part of the basin have bias relatively close to zero suggesting good performance of the uncorrected CMORPH product. However, relatively large negative bias values (-20 %) are shown in the Upper Zambezi‘s high elevated areas such as Kabompo and northern Barotse Basin, in the south-eastern part of the basin such as Shire River Basin and in in the Lower Zambezi’s downstream areas where the Zambezi River enters the Indian Ocean. CMORPH overestimates rainfall locally in Kariba, Luanginga, and Luangwa basins by positive bias values. As such CMORPH estimates do not consistently provide results that match rain gauge observations. Since CMORPH estimates have pronounced error (-10 > bias (%) > 10), bias needs to be removed before the product can be applied for hydrological analysis and in water resources applications. Figure 2 also shows contours for rain gauge mean annual precipitation (MAP) in the Zambezi Basin with higher values in the northern parts of the basin (Kabompo and Luangwa) compared to localised estimates of MAP such as in Shire River and Kariba sub-basins.

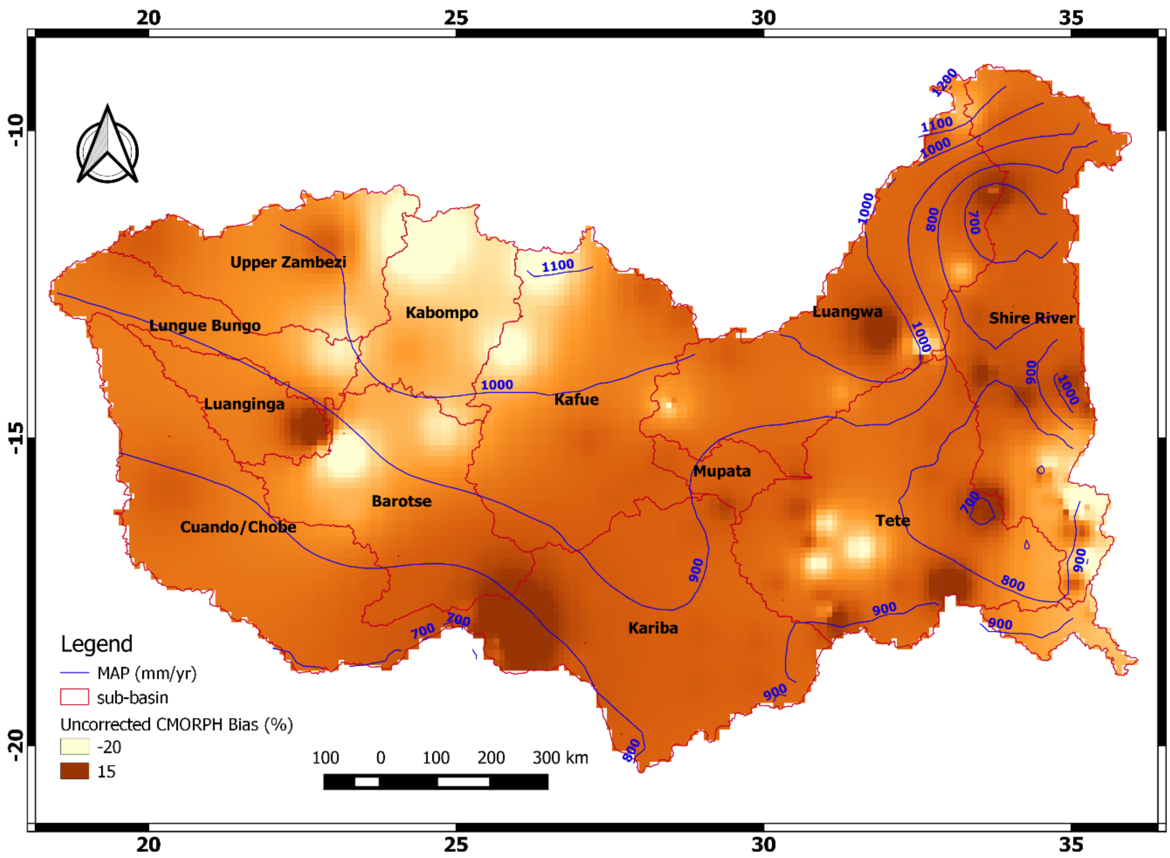

Figure 2: The spatial variation of bias (%) for gauge vs uncorrected CMORPH daily rainfall (1998-2013) for the Zambezi Basin. The gauge based isohyets for Mean Annual Precipitation (MAP) are shown in blue.

4.2. Effects of elevation and distance from large-scale open water bodies on CMORPH bias

Figure 3 shows Taylor diagrams with a comparison of basin lumped estimates of daily uncorrected time series (1999–2013) of CMORPH and gauge based rainfall for the 3 elevation zones (left panes) and 4 distance zones from large-scale open water bodies (right panes). Here CMORPH performance is indicated by means of the root mean square difference (*E*), correlation coefficient (*R*) and standard deviation. Figure 3 shows that standard deviations in the elevation zones and the distance zones (except for the < 10 km distance zone) are lower than the reference/rain gauge standard deviation which is indicated by the black arc (value of 8.45 mm/day). The stations in the high elevation zone (> 950 m) and long distance zone (> 100 km) reveal lower variability than stations at lower elevation and shorter distance zones. With respect to the reference line, CMORPH estimates that are lumped for respective elevation zones and distance to a large water body do not match standard deviation of rain gauge based counterparts. Figure 3 also shows that CMORPH standard deviations that are close to gauge based rainfall belong to lower elevation and shorter distance zones. Based on the Taylor diagrams, the statistics (R and E) for uncorrected CMORPH show increasing performance for increasing elevation and increasing distance from large-scale water bodies. Specifically, stations in the lower elevation zones (< 250m) have lower R and higher E than the higher elevation zones (> 950 m). For shorter distance zones lower R and and higher E is shown than for longer distance zones (> 100 km). These findings suggest that in genral effects of distance to large scale water body are minimal except for distances <10 km.

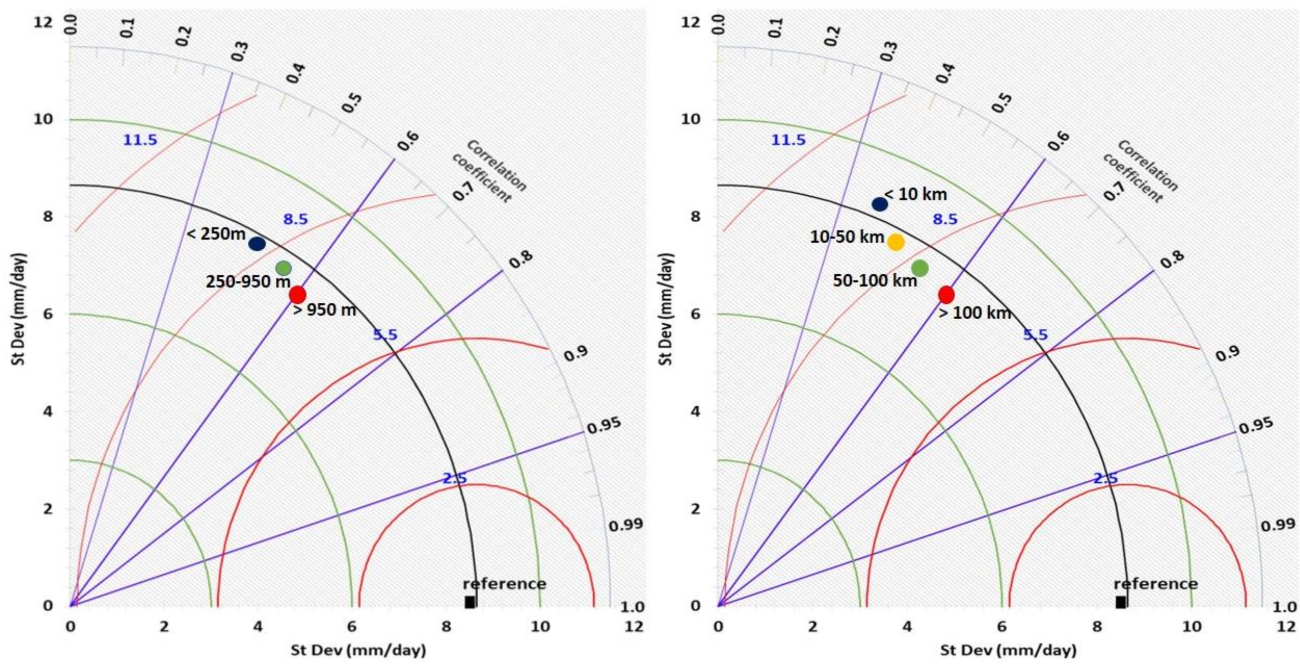

a) Elevation zones b) Distance zones

Figure 3. Time series of rain gauge (reference) vs CMORPH estimations, period 1999-2013, for elevation zones (left panes) and distance zones (right panes) in the Zambezi Basin. The correlation coefficients for the radial line denote the relationship between CMORPH and gauge based observations. Standard deviations on both the x and y axes show the amount of variance between the two-time series. The standard deviation of the CMORPH pattern is proportional to the radial distance from the origin. The angle between symbol and abscissa measures the correlation between CMORPH and rain gauge observations. The root mean square difference (red contours) between the CMORPH and rain gauge patterns is proportional to the distance to the point on the x-axis identified as "reference”. For details, see Taylor (2001).

4.3. Evaluation of bias correction

4.3.1. Standard statistics

Figure 4 shows frequency based statistics (mean and maximum) on accuracy of CMORPH rainfall estimates for each bias correction method. The ratio of cumulated estimates (1999-2013) from rain gauge and CMORPH estimates for the Lower, Middle and Upper Zambezi sub-basins are shown. Results show that the bias of CMORPH moderately reduced for each of the five bias correction schemes. However, the effectiveness of the schemes vary spatially with best performance in Lower and Upper Zambezi sub-basin and relatively poor performance in the Middle Zambezi sub-basin (see Figure 4).

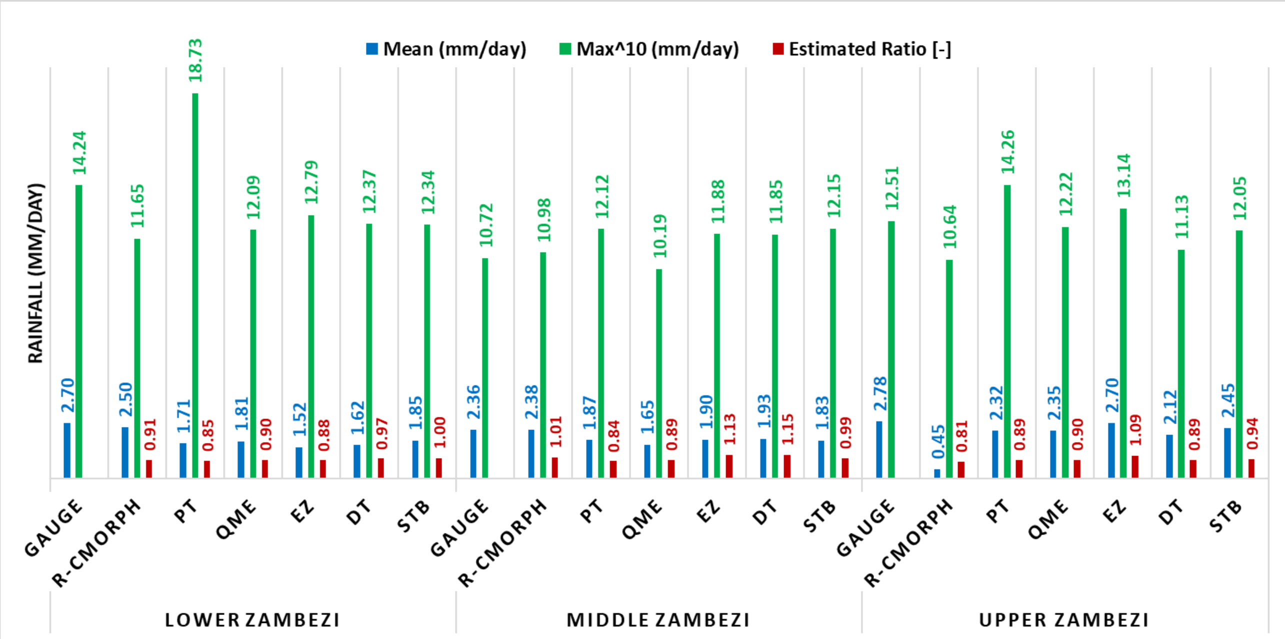

Figure 4: Frequency based statistics (mean, max and estimated ratio of gauged sum vs CMORPH sum for 1999-2013) of corrected CMORPH for Lower, Middle and Upper Zambezi Basin.

Judging by the three performance indicators (mean, max and estimated ratio), results indicate that STB bias correction scheme is consistently effective in removing CMORPH rainfall bias in the Zambezi Basin. STB and PT effectively adjust for the mean of CMORPH rainfall estimates. Statistics in Figure 5 confirm these findings especially for the Upper Zambezi sub-basin where the mean of corrected estimates improved by > 60 % from the mean of uncorrected estimates. In addition, PT in the Lower Zambezi, QME in both Middle and Upper Zambezi and STB in the Upper Zambezi were also effective (improvement by 16 %) in correcting for the highest values in the rainfall estimates. STB performs better than other bias schemes in reproducing rainfall for the Lower and Upper Zambezi sub-basin, where the ratio of gauge total to corrected CMORPH total is close to 1.0.

Figure 5 shows the mean absolute error (MAE) and percentage bias (% bias) on the left axis and Nash Sutcliffe Efficency (NSE) on the right axis as measures to evaluate performance of bias correction schemes in the Zambezi Basin. The effectiveness of the bias correction by all schemes varies over the different parts of the basin but is higher in the Lower and Upper

Zambezi than in the Middle Zambezi. The STB, PT and EZ shows improved performance by exhibiting smaller MAEs compared to the uncorrected CMORPH (R-CMORPH). A greater improvement is shown for the Middle Zambezi where the uncorrected MAE of 1.89 mm/day is reduced to 0.86 mm/day after bias correction by the elevation zone bias correction scheme (EZ). The signal on improved performance for the Lower and Middle Zambezi as compared to the Upper Zambezi is also evident for the majority of the bias correction techniques. However, relatively large error remains in the MAE.

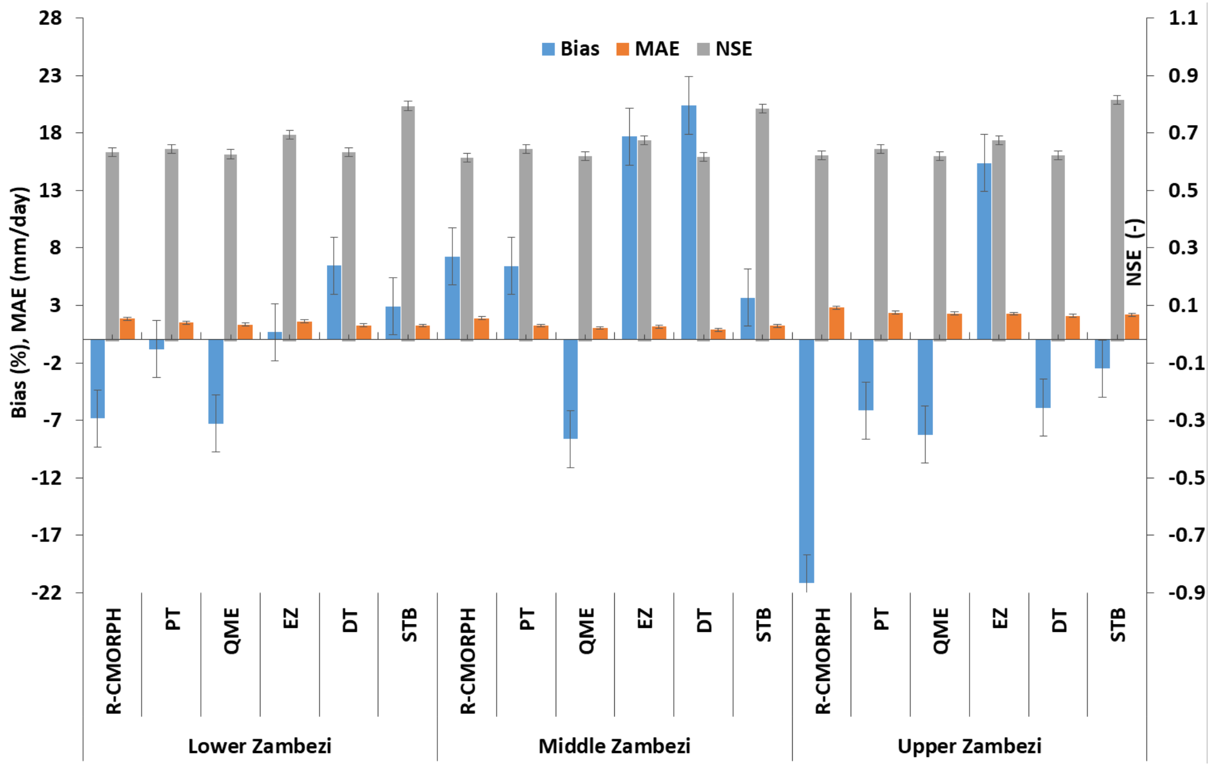

Figure 5: Percentage bias, Mean Absolute Error (left axis) and Nash Sutcliffe (NSE) (right axis) of corrected and uncorrected CMORPH (R-CMORPH) daily rainfall averaged for the Lower Zambezi, Middle Zambezi and Upper Zambezi. (put NSE to the right of the numbers)

NSE for STB is above 0.8 for all three Zambezi sub-basins. This is followed by EZ with NSE above 0.7 for the three sub-basins. The lowest NSE is for QME which is close to 0.65 for all three sub-basins. Best results for reducing bias (% bias) are obtained by EZ in the Lower Zambezi (% bias of 0.7 % ~ absolute bias of 0.10 mm/day) and Upper Zambezi (0.22 % ~0.23 mm/day), PT in the Lower and Middle Zambezi (-0.84 % ~0.18 mm/day) and STB in all the basins (< 3.70 % ~0.24 mm/day). Gao and Liu (2013) over the Tibetan Plateau asserts that EZ is valuable in correcting systematic biases to provide a more accurate precipitation input for rainfall-runoff modelling. Significant underestimation for the uncorrected (-21.16 % ~0.44 mm/day) and for bias corrected CMORPH are shown for the Upper Zambezi sub-basin.

4.3.2. *Significance testing*

Table 2 shows results of statistical tests to assess whether there is a significant difference ($p < 0.05$) between rain gauge vs uncorrected and bias corrected CMORPH satellite rainfall for each of the 52 rain gauge stations. Results are summarised for the Upper, Middle and Lower Zambezi and in the Zambezi basin. The null hypothesis is rejected for PT (Lower Zambezi), DT (Upper Zambezi) and QME (all the 3 sub-basins) since $p < 0.05$. This means that statistically the above mentioned bias correction schemes results deviate from the gauge. The null hypothesis is accepted for STB and EZ (all three sub-basins), DT (Lower and Upper Zambezi) and PT (Middle and Upper Zambezi), since $p > 0.05$ showing the effectiveness of these bias correction schemes. Compared to uncorrected satellite rainfall (R-MORPH), results also reveal that the bias corrected satellite rainfall is closer to the gauge based rainfall.

Table 2: Paired t-tests for the Upper, Middle and Lower Zambezi. The mean difference is significant at the 0.05 level. Bold shows significant values..

Basin	Rainfall Estimate	t-value	Mean Std. Error	p-value (0.05)
Lower Zambezi	R-CMORPH	8.95	0.04	**0.04**
	DT	39.86	0.09	0.35
	PT	21.08	0.04	**0.03**
	QME	23.99	0.04	**0.04**
	EZ	36.43	0.03	0.27
	STB	14.7	0.04	0.46
Middle Zambezi	R-CMORPH	3.27	0.03	**0.001**
	DT	41.9	0.07	0.24
	PT	26.02	0.03	0.14
	QME	18.38	0.03	**0.00**
	EZ	26.60	0.02	0.07
	STB	23.6	0.03	0.09
Upper Zambezi	R-CMORPH	4.28	0.08	**0.00**
	DT	22.63	0.14	**0.01**
	PT	12.98	0.07	**0.05**
	QME	13.27	0.07	**0.00**
	EZ	13.73	0.07	0.14
	STB	13.62	**0.07**	**0.08**

4.3.3. *Analysis of variance (ANOVA test)*

The ANOVA test is similar to a t-test except that the test was used to compare mean values from three or more data samples. Results of ANOVA shows that there is a significant ($p < 0.05$) difference in the mean values of the 5 bias correction results across the three sub-basins. This warranted the running of a post-hoc test to determine which schemes differ significantly. The contingency matrix in Table 2 shows results of the post-hoc test results summarized for the Tukey HSD, Schefe and the Bonferroni methods but also for the Upper, Lower and Middle Zambezi. Table 3 also show that STB, PT and EZ are significantly different from the distribution transformation technique (DT) for the three sub-basins. STB, the best performing bias correction scheme identified using majority of the indicators, is also significantly different from QME and EZ. QME which has poorly performed is significantly different from EZ. Results are important for further application of the bias correction schemes for studies such as flood, drought and water resources modelling.

Table 3: ANOVA post-hoc tests for the results of the five bias correction schemes ($p<0.05$). The checklist table gives a indication (symbol) where two bias correction scheme's results are significantly different from each other. Where there is no symbol, it means that the schemes' results are not significantly different. The different symbols represent the Upper, Middle and Lower Zambezi basins.

	STB	PT	QME	DT	EZ
STB			√	x √ 💡	√
PT			💡	x √ 💡	
QME	√				💡
DT	x √ 💡	x √ 💡	x √		x 💡
EZ	√			x √ 💡	
	Key	x	Upper Zambezi		
		√	Lower Zambezi		
		💡	Middle Zambezi		

4.3.4. Taylor Diagrams

Figure 6 shows the Taylor diagram for time series of rain gauge (reference) observations vs CMORPH bias correction schemes averaged for the Lower Zambezi (UZ), Middle Zambezi (MZ) and Upper Zambezi (UZ). Absolute values used to develop the Taylor diagram are shown in Appendix 2. The position of each bias correction scheme and uncorrected satellite rainfall (R-MORPH) on Figure 6 shows how closely the rainfall by uncorrected CMORPH (R-MORPH) matches rain gauge observations as well as effectiveness of each of the bias schemes. Overall, all bias correction schemes show intermediate performance in terms of bias removal. Only the PT and STB for the Lower Zambezi sub-basin lie on the line of standard deviation (brown dashed arc) and means the standard deviation of the data for the two bias correction schemes match the gauge observations. This also indicates that rainfall variations after PT and STB bias correction for the Lower Zambezi resembles gauge based standard deviation. Note however that STB performs better than EZ as shown by the superior correlation coefficient. Compared against the reference line of mean standard deviation (8.5 mm/day), the rainfall standard deviation for most bias correction schemes is below this line and as such exhibit low variability across the Zambezi Basin.

Figure 6 also shows that most of the bias correction schemes have standard deviation range of 6.0 to 8.0 mm/day. There is a consistent pattern between the bias correction schemes that have low R and high RMSE difference indicating that these schemes are not effective in bias removal. Overall, the best performing bias correction schemes (STB and EZ) have R > 0.6, standard deviation relatively close to the reference point and RMSE < 7 mm/day. The uncorrected CMORPH (R-MORPH) lies far away from the marked reference (gauge) point on the x-axis suggesting an intermediate overall effectiveness of the bias correction schemes such as STB, EZ, DT and PT in removing error as they are relatively closer to the marked reference point.

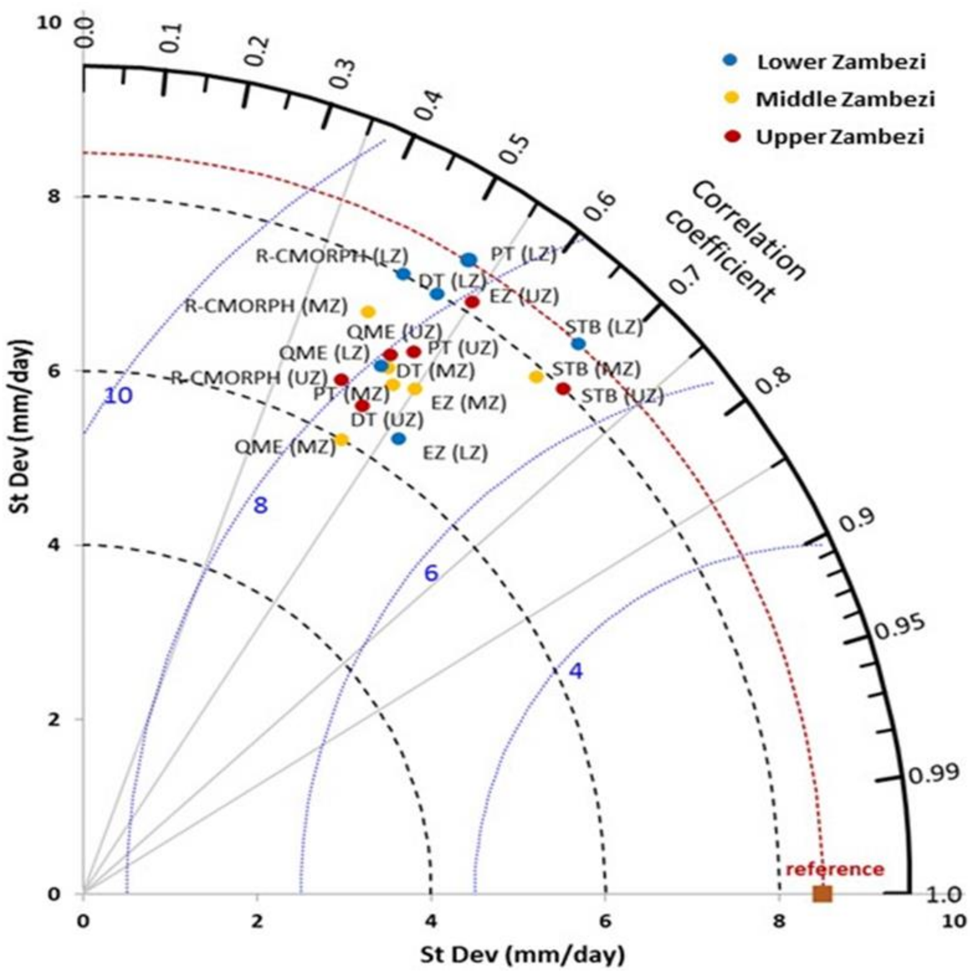

Figure 6: Taylor's diagram on Rain gauge (reference) observations and CMORPH bias corrected estimates (all 5 schemes) as averaged for the Lower Zambezi (LZ), Middle Zambezi (MZ), and Upper Zambezi (UZ) for the period 1999-2013. The distance of the symbol from point (1, 0) is also a relative measure of the bias correction scheme perfromance. The position of each symbol appearing on the plot quantifies how closely precipitation estimates by respective bias correction scheme's matches counterparts by rain gauge. The dashed blue lines indicate the root mean square difference (mm/day).

The least performing bias correction scheme is QME with relatively large RSMD (> 8 mm/day) and with low R (< 0.49) and standard deviation (< 6.5 mm/day). Inherent to the methodology of most of bias correction schemes (e.g. QME) is that the spatial pattern of the SRE does not change and therefore R for a specific station for daily precipitation does not necessarily improve. The bias correction results by the Taylor Diagram in Figure 6 corroborates with findings shown in Figure 4 and Figure 5 for mean, max, ratio of rainfall totals and bias as performance indicators.

4.3.5. q-q plots

Figure 7 shows q-q plots for the Upper, Middle and Lower Zambezi for gauge rainfall against uncorrected and bias corrected CMORPH rainfall. Results show that the STB q-q plots for bias corrected CMORPH across the 3 basins has majority of points that fall approximately along the 45-degree reference line. This means that the STB bias corrected satellite rainfall has closer distribution to the rain gauge as compared to the uncorrected CMORPH counterparts suggesting effectiveness of the bias correction scheme. Other bias correction schemes such as QME, EZ and PT have data points showing a greater departure from the 45-degree reference line so performance is less effective.

In some instances in both the Upper, Middle and Lower Zambezi, bias corrected values are significantly higher than the corresponding gauge values whereas in some instances there is serious underestimation. All q-q plots also show that for all bias correction schemes, the differences between gauge and satellite rainfall are smallest for low rainfall rates (< 2.5 mm/day) and increasing for heavy rainfall (> 20.0 mm/day). In more detail, all the bias correction schemes show a larger difference for the transition area from low to heavy rainfall. QME and PT are not in good agreement with the rest of the bias correction schemes for higher rainfall estimates (40 and 60 mm/day).

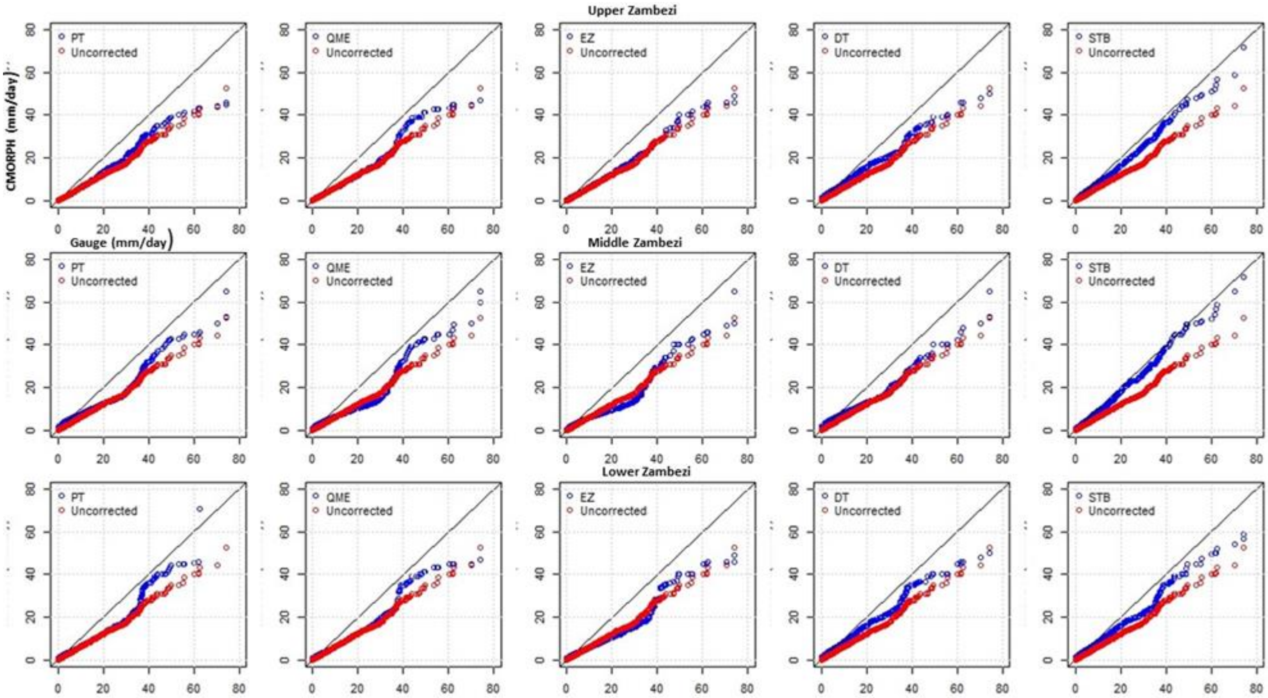

Figure 7: q-q plot for gauge vs satellite rainfall (corrected and bias corrected) for the Upper (top panes), Middle (middle panes) and Lower (bottom panes) Zambezi.

4.3.6. CMORPH rainy days

Occurance (%) of rainfall rates in the Zambezi Basin for each bias correction scheme is shown in Figure 8. The highest percentage (80-90 %) is shown for very light rainfall (0.0-2.5 mm/day). A smaller percentage is shown for 2.5-5.0 mm/day which is the light rainfall class. Smallest percentage (< 5%) is shown for heavy rainfall (> 20.0 mm/day). The CMORPH rainfall corrected with STB, PT and DT matches the gauge based rainfall (%) in the Lower, Middle and Upper Zambezi suggesting good performance. All five bias correction schemes in the Zambezi Basin generally tend to overestimate low rainfall (< 2.5 mm/day). There is a small difference for moderate rainy days classification of 10.0-20.0 mm/day. For QME in the Middle and Upper Zambezi, there is overestimation by > 80 %. There is underestimation of rainfall greater than 20 mm/day.

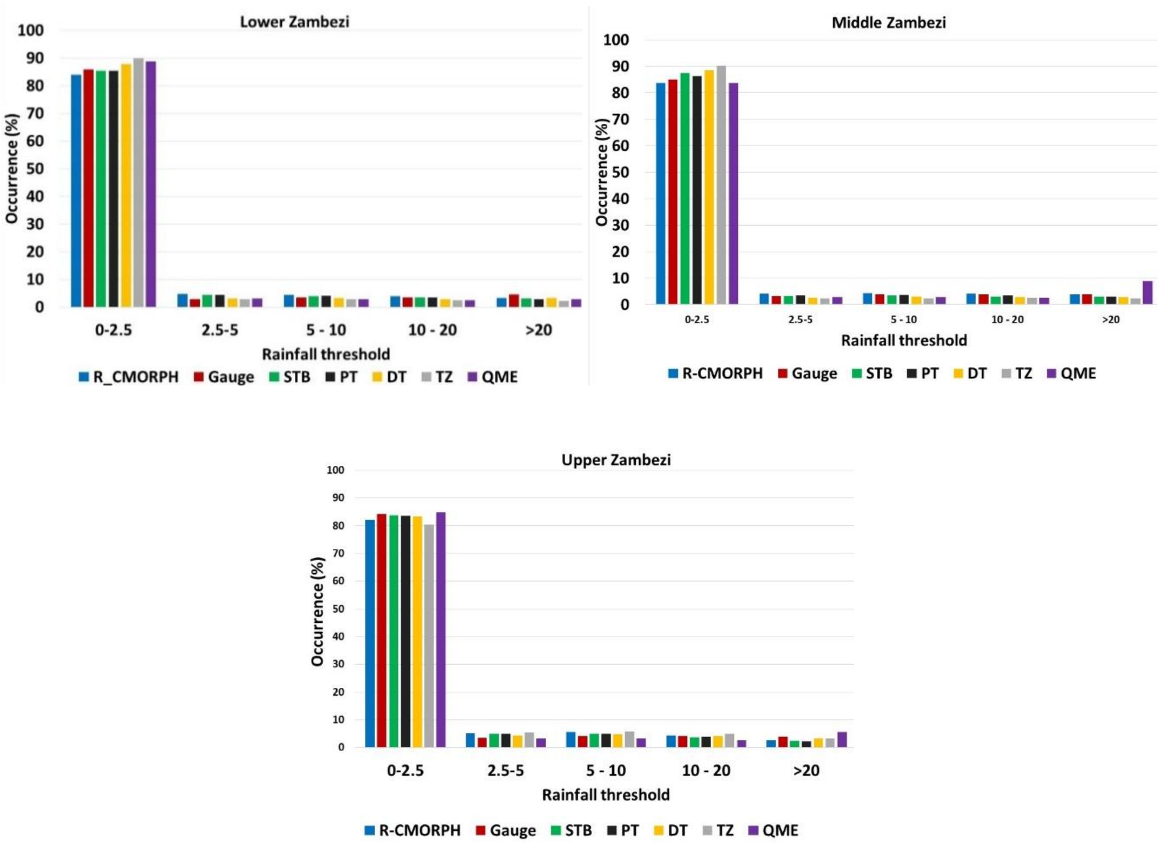

Figure 8: Percentage occurance for rainfall rate classes

Figure 9 gives the bias correction performance for the different rainy day classes. Results of bias removal varies for the Lower, Middle and Upper Zambezi. Comparatively, the STB and EZ show effectiveness in bias removal with an average bias correction of 0.97 % and 3.6 % in the whole basin respectively. Results show more effectiveness in reducing the percentage bias for light rainfall and moderate rainfall (0-2.5 and 5.0-10.0 mm/day) than the high to very high rainfall (10.0-20.0 mm/day and >20.0 mm/day) across the whole basin.

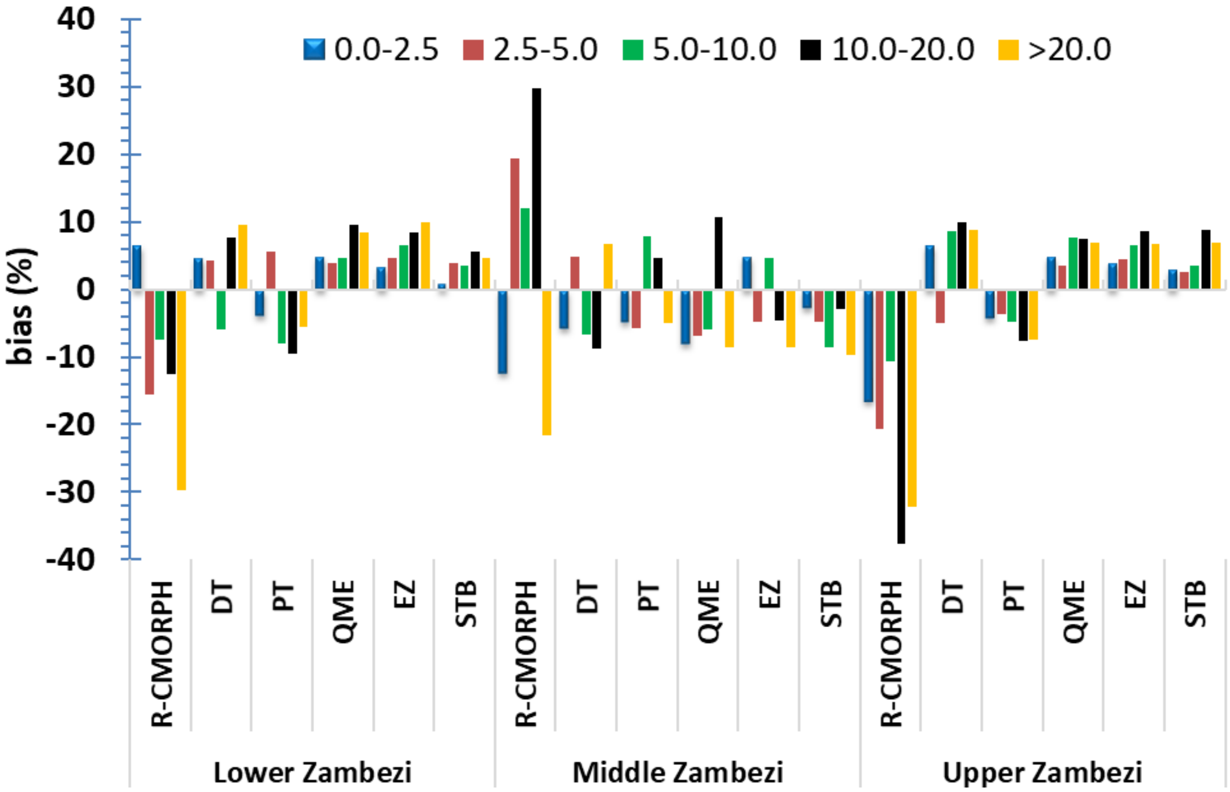

Figure 9: Bias correction (%) for respective rainfall rate classes

4.4. Spatial cross-validation

Table 4 shows the cross-validation results on bias correction for 8 rain gauge stations in the wet and dry seasons. It is evident that CMORPH has a considerable bias, although this bias is not always consistent for all 8 validation stations. Overall, Mutarara station has the highest positive bias (overestimation) whereas Makhanga has the highest negative bias (underestimation) for uncorrected CMORPH. Bias is effectively being removed by the STB followed by the EZ bias correction schemes. Bias is more effectively removed for the wet season than for the dry season. For the dry season, the STB shows good performance for Mkhanga and Nchalo stations, whereas good performance is shown for Kabompo and Chichiri stations. However, the MAE is higher for the wet season than for the dry season. Correlation coefficient for bias corrected satellite rainfall is higher for the wet season than for the dry season.

Table 4: Cross validation results for the bias correction procedure with 8 gauging stations for the dry and wet season. Stations lie at average elevation zone and sort of centred in an elevation zone. R-Morph is the uncorrected R-CMOPRPH estimate. DT, PT, QME, EZ and STB are the bias corrected rainfall estimate. Bold values indicate best performance. * = zone 1: elevation of < 250 m , ** = zone 2: elevation range of 250 - 950 m and *** = zone 3: elevation > 950 m

		Dry Season (April-Sept)				Wet Season (Oct-March)			
Station	Rainfall Estimate	Bias (%)	MAE	Correlation	Estimated Ratio	Bias (%)	MAE	Correlation	Estimated Ratio
Makhanga*	R-CMORPH	-28.69	1.23	0.42	0.87	-21.17	8.63	0.43	0.91
	DT	-1.37	0.53	0.56	0.99	-1.66	3.96	0.65	0.94
	PT	-5.62	0.52	0.54	0.95	-3.5	4.67	0.64	1.02
	QME	1.98	0.54	0.54	0.95	-0.64	4.86	0.65	0.97
	EZ	2.10	0.47	0.55	1.03	-0.11	4.08	0.58	0.96
	STB	0.77	0.61	0.56	1.04	0.5	5.06	0.62	1.02
Nchalo*	R-CMORPH	-33.05	1.13	0.42	0.84	-25.18	8.05	0.38	0.83
	DT	-0.23	0.73	0.56	0.96	-2.61	3.65	0.50	0.87
	PT	-4.28	0.68	0.54	0.93	-6.48	5.05	0.59	0.92
	QME	1.90	0.72	0.53	0.81	-0.56	5.29	0.53	0.91
	EZ	0.35	0.63	0.54	0.99	**0.22**	4.4	0.60	1.06
	STB	-0.43	0.73	0.58	0.96	-1.23	5.54	0.61	1.02
Rukomichi**	R-CMORPH	-23.05	0.93	0.42	0.86	-21.18	6.69	0.31	0.73
	DT	-0.23	0.90	0.56	0.94	-6.2	3.51	0.60	0.87
	PT	-4.28	0.73	0.54	0.93	-2.48	3.62	0.59	0.92
	QME	1.90	0.75	0.53	1.03	-0.56	3.88	0.54	0.83
	EZ	0.35	0.71	0.54	0.99	**0.22**	3.5	0.60	1.06
	STB	-0.43	0.76	0.58	0.94	-1.26	3.33	0.61	1.02
Mutarara**	R-CMORPH	20.15	0.24	0.49	1.10	20.1	2.34	0.50	1.05
	DT	11.4	0.18	0.60	1.03	8.7	1.23	0.63	1.04
	PT	8.4	0.12	0.55	0.91	4.3	1.28	0.68	1.03
	QME	5.7	0.14	0.63	1.1	8.1	1.4	0.65	0.98
	EZ	-12.8	**0.09**	0.54	0.95	1.9	1.23	0.69	1.03
	STB	4.5	0.14	0.53	1.1	2.1	1.33	**0.73**	**1.01**
Mfuwe**	R-CMORPH	40.2	0.28	0.45	0.85	35.4	6.4	0.48	1.08
	DT	2.9	0.62	0.53	0.96	4.6	3.9	0.62	0.98
	PT	3.7	0.22	0.55	0.92	7.9	5.25	0.65	0.96
	QME	3.9	0.30	0.55	0.93	5.4	5.68	0.64	0.97
	EZ	6.1	0.24	0.54	0.92	3.8	5.18	0.56	0.98
	STB	5.4	0.26	0.65	0.93	1.2	4.66	0.65	0.96
Kabombo***	R-CMORPH	25.3	0.70	0.44	0.95	24.3	3.8	0.48	0.85
	DT	7.7	0.32	0.51	0.96	5.7	3.5	0.62	0.94
	PT	9.2	0.13	0.54	1.10	8.7	3.0	0.64	0.96
	QME	2.7	0.32	0.62	1.10	2.8	3.2	0.63	0.95
	EZ	5.6	0.22	0.53	0.91	3.3	2.7	0.54	0.96
	STB	19	0.13	0.62	1.01	9.3	2.7	0.64	0.93

Chichiri***	R-CMORPH	34.5	1.56	0.47	0.8	-37.3	4.7	0.45	0.84
	DT	12.2	0.60	0.51	0.85	5.5	3.2	0.51	0.93
	PT	9.4	0.42	0.52	1.04	-7.8	4.1	0.54	0.95
	QME	8.4	0.92	0.56	1.05	-13.0	4.1	0.64	1.04
	EZ	-13	0.61	0.60	0.94	-9.9	4.2	0.60	0.96
	STB	3.2	0.45	0.63	0.98	-14.3	2.1	0.65	**0.99**
Chitedze***	R-CMORPH	41.5	0.90	0.47	1.06	42.3	5.4	0.48	0.89
	DT	16.7	0.53	0.54	0.98	-13.2	3.3	0.62	0.86
	PT	-16.5	0.44	0.55	0.99	22.2	4.5	0.65	1.05
	QME	18.2	0.41	0.57	1.04	18.5	4.3	0.64	1.04
	EZ	11.7	0.32	0.57	1.02	8.4	4.6	0.55	1.03
	STB	3.9	0.23	0.60	0.03	-8.2	3.7	0.65	0.97

4.5. Temporal cross-validation

The same performance indicators in spatial cross-validation are calculated for the temporal cross-validation. Results are presented in Table 5. The MAE is higher for the wet season than for the dry season. The difference in effectiveness in the error removal between the dry and wet season is much larger. STB outperforms both bias correction methods but does also have problems correcting the estimated ratios. After the correction, the correlation coefficient is much improved. The fact that MAE remains relatively large indicates that errors remain locally large. These values are almost in same range to performance indicators obtained from the main performance assessment period (1999-2013). The estimated ratio shows improvement for the Middle Zambezi than for the Lower and Upper Zambezi.

Table 5: Temporal-cross validation results for the period 1998-1999 for the wet and dry season

		Dry Season (April-Sept)				Wet Season (Oct-March)			
	Rainfall Estimate	Bias (%)	MAE	Correlation	Estimated Ratio	Bias (%)	MAE	Correlation	Estimated Ratio
Lower Zambezi	R-CMORPH	-28.26	1.10	0.42	0.86	-22.51	7.79	0.37	0.82
	DT	-0.61	0.72	0.56	0.96	-3.49	3.71	0.58	0.89
	PT	-4.73	0.64	0.54	0.94	-4.15	4.45	0.61	0.95
	QME	1.93	0.67	0.53	0.93	-0.59	4.68	0.57	0.90
	EZ	0.93	0.60	0.54	1.00	0.11	3.99	0.59	1.03
	STB	-0.03	0.70	0.57	0.98	-0.66	4.64	0.61	1.02
Middle Zambezi	R-CMORPH	28.55	0.41	0.46	0.97	26.60	4.18	0.49	0.99
	DT	7.33	0.37	0.55	0.98	6.33	2.88	0.62	0.99
	PT	7.10	0.16	0.55	0.98	6.97	3.18	0.66	0.98
	QME	4.10	0.25	0.60	1.04	5.43	3.43	0.64	0.97
	EZ	-0.37	0.18	0.54	0.93	3.00	3.04	0.60	0.99

	STB	9.63	0.18	0.60	1.01	4.20	2.90	0.67	0.97
	R-CMORPH	38	1.23	0.47	0.93	2.5	5.05	0.465	0.865
	DT	14.45	0.565	0.525	0.915	-3.85	3.25	0.565	0.895
Upper	PT	-3.55	0.43	0.535	1.015	7.2	4.3	0.595	1
Zambezi	QME	13.3	0.665	0.565	1.045	2.75	4.2	0.64	1.04
	EZ	-0.65	0.465	0.585	0.98	-0.75	4.4	0.575	0.995
	STB	3.55	0.34	0.615	0.505	-11.25	2.9	0.65	0.98

5. Discussion

We present methods to assess the performance of bias correction schemes for CMORPH rainfall estimates in the Zambezi River Basin. For correction we applied sequential windows of 7 days that count 5 rainy days with rainfall threshold of 5 mm. First we aimed to evaluate if performance of CMORPH rainfall is affected by elevation and distance from large scale open water bodies. Results in Taylor diagrams show that effects of distances > 10 km are minimal in this study. For distance < 10 km results in the same Taylor diagrams shows some effect with increased CMORPH estimation errors although not clearly identifiable by the limited number of gauging stations at distance < 10 km. We advocate further study on this aspect since the gauge network we relied on was not specifically designed for this purpose of analysis.

For elevation, Romilly and Gebremichael (2011) showed that the accuracy of CMORPH at monthly time base is related to elevation for six river basins in Ethiopia. A similar finding was reported by Haile et al. (2009), Katiraie-Boroujerdy et al., (2013), Rientjes et al. (2013a) and Wu and Zhai (2012) who found that performance of CMORPH is affected by elevation. Contrary to these findings, Vernimmen et al. (2012) concluded that TRMM Multi-satellite Precipitation Analysis (TMPA) 3B42RT performance was not affected by elevation (R^2 = 0.0001) for Jakarta, Bogor, Bandung, Java, Kalimantan and Sumatra regions (Indonesia). The study by Gao and Liu (2013) showed that the bias in CMORPH rainfall over the Tibetan Plateau is affected by elevation. Whilst distance from large scale open water bodies and elevation have been assessed separately for this study, Habib et al. (2012a) revealed that both aspects interact in the Nile Basin to produce unique circulation patterns to affect the performance of SRE.

Second we evaluate the effectiveness of linear/non-linear and time-space variant/invariant bias correction schemes. The bias correction results by means of performance indicators such as Taylor Diagrams, q-q plots, ANOVA and standard statistics such as mean, max, ratio of rainfall totals and bias reveal that the STB is the best bias correction method. This method by its nature, consider correction only for spatial distributed patterns in bias, commonly known as space variant/invariant and thus forces the estimates to behave as observations. We did not investigate effects of the applied sequential windows of 7 days for each bias correction scheme but note that other window lenghts could yield more favarable results for bias schemes such as PT, DT and QME that commomnly rely on larger sample sizes. As alluded to by Habib (2013), correction should improve hydrological applications by improved rainfall representation. This applies to Zambezi basin as well with demands for applications of the product such as for drought analysis, flood prediction, weather forecasting and rainfall runoff modeling. The study is unique as we assess the importance of space and time aspects of CMORPH bias for rainfall-runoff modeling in a data scarce catchment. Findings in this study on cross and temporal validation contribute to efforts that aim towards enhancing the real-world applicability of satellite rainfall products. The study site is the Zambezi Basin-an example of many world regions that can benefit from satellite-based rainfall products for resource assessments and monitoring.

Thirdly, an assessment of the performance of bias correction schemes to represent different rainfall rates and climate seasonality is presented. Our findings show that bias is most overestimated for the very light rainfall (< 2.5 mm/day), which is also the range that shows the best bias reduction, which in turn is most effective during the wet season. Results also show that there is underestimation of rainfall greater than 20 mm/day. The poor performance of correction for the heavy rainfall class is caused by, sometimes, large mismatch of high rain gauge values versus low CMORPH values. This leads to unrealistically high CMORPH values which remain poorly corrected by bias schemes. Results are consistent with findings by Gao and Liu (2013) in the Tibetan Plateau who also found consistent under and overestimation of occurence by CMORPH for rainfall rates >10.0 mm/day. A study by Zulkafli et al. (2014) in French Guiana and North Brazil noted that the low sampling frequency and consequently missed short-duration precipitation events between satellite measurements results in underestimation, particularly for heavy rainfall.

Lasty, spatial and temporal cross validation reveal effectiveness of bias correction schemes. The hold-out sample of 8 stations in this work showed the applicability of different bias correction methods under different geographical space (spatial). There is improved performance of satellite rainfall for the wet season than for the dry season based on correlation coefficient and MAE. The study by Ines and Hansen (2006) for semi-arid eastern Kenya showed that multiplicative bias correction schemes such as STB were effective in correcting the total of the daily rainfall grouped into seasons. Our results show that effectiveness in bias removal in the wet season is higher than in the dry season. This is contrary to Vernimmen et al. (2012) who showed that for the dry season, bias for PT decreased in Jakarta, Bogor, Bandung, East Java and Lampung regions after bias correction of monthly TMPA 3B42RT precipitation estimates over the period 2003–2008. Habib (2014) evaluated sensitivity of STB for the dry and wet season and concluded that the bias correction factor for CMOPRH shows lower sensitivity for the wet season as compared to the dry season. Our findings also reveal that bias factors for all the schemes are more variable in the dry season than in the wet season and lead to poor performance of the bias correction schemes in the dry season.

6. Conclusions

In this study four conclusions are drawn:

1. Analysis on gauge and CMORPH rainfall estimates shows that performance increases for higher elevation (>950 m) in the Zambezi Basin and that CMORPH has largest mismatch at low elevation. Such analysis was established for rain gauges within elevation classes of < 250 m, 250 - 950 m and > 950 m. The match between gauge and CMORPH estimates improved at increasing distance to large-scale open water bodies. This was established for rain gauges located within specified distances of 10 -50 km, 50 -100 km and > 100 km to a large scale open water body. For distances < 10 km errors by CMORPH increased but we advocate further study with specifically designed gauging network for the research purpose.

2. For each of the five bias correction methods applied, accuracy of the CMORPH satellite rainfall estimates improved. Assessment through standard statistics, Taylor Diagrams, t-tests, ANOVA and q-q plots shows that STB that accounts for space and time variation of bias, is found more effective in reducing rainfall bias in the basin than the rest of the bias correction schemes. This indicates that the temporal aspect of CMORPH bias is more important than the spatial aspect in the Zambezi Basin. Quantile-quantile (q-q) plots for all the bias correction schemes in general show that bias corrected rainfall is in good agreement

with gauge based rainfall for low rainfall rates but that high rainfall rates are largely overestimated.

3. Differences in the mechanisms that drive precipitation throughout the year could result in different biases for each of the seasons, which motivated us to calculate the bias correction factors for dry and wet seasons separately. As such CMORPH rainfall time series were divided to assess the influence of seasonality on performance of bias correction schemes. Overal, the bias correction schemes reveal that bias removal is more effective in the wet season than in the dry season.

4. We assessed whether bias correction varies for different rainfall rates of daily rainfall in the Zambezi Basin. There is overestimation of very light rainfall (< 2.5 mm/day) and underestimation of very heavy rainfall (>20 mm/day) after application of the bias correction schemes. Bias was more effectively reduced for very low to moderate rainfall (< 2.5 and 5.0-10.0 mmm/day) than for high to very high rainfall (10.0-20.0 mm/day and >20.0 mm/day). Overall, the STB and EZ more consistently removed bias in all the rainy days classification compared to the three other bias correction schemes. Effects of length of sequential window sizes for selected bias correction schemes is not investigated but different length possibly could yield more favourable results for PT, QME and DT bias correction schemes.

Analysis serve to improve reliability of SREs applications in hydrological analysis and water resource applications in the Zambezi basin such as in drought analysis, flood prediction, weather forecasting and rainfall runoff modelling. In follow-up studies, we aim at hydrologic evaluation of bias corrected CMORPH rainfall estimates at the headwater catchment of the Zambezi River.

Acknowledgements

The study was supported by WaterNet through the DANIDA Transboundary PhD Research in the Zambezi Basin and the University of Twente's ITC Faculty. The authors acknowledge the University of Zimbabwe's Civil Engineering Department for platform to carry out this research.

Author Contributions

Webster Gumindoga was responsible for the development of bias correction schemes in the Zambezi basin and research approach. Tom Rientjes and Alemseged Haile were responsible for synthesising the methodology and made large contributions to the manuscript write-up. Hodson Makurira provided some of the rain gauge data and related findings of this study to previous work in the Zambezi Basin. Reggiani Paulo assisted in interpretation of bias correction results.

Conflict of Interests

The authors declare no conflict of interests.

References

Beilfuss, R., Dutton, P., and Moore, D.: Landcover and Landuse change in the Zambezi Delta, in: Zambezi Basin Wetlands Volume III Landuse Change and Human impacts, Chapter 2, Biodiversity Foundation for Africa, Harare, 31-105, 2000.

Beilfuss, R.: A Risky Climate for Southern African Hydro: Assessing hydrological risks and consequences for Zambezi River Basin dams, 2012.

Beyer, M., Wallner, M., Bahlmann, L., Thiemig, V., Dietrich, J., and Billib, M.: Rainfall characteristics and their implications for rain-fed agriculture: a case study in the Upper Zambezi River Basin, Hydrological Sciences Journal, null-null, 10.1080/02626667.2014.983519, 2014.

Bitew, M. M., and Gebremichael, M.: Evaluation of satellite rainfall products through hydrologic simulation in a fully distributed hydrologic model, Water Resources Research, 47, 2011.

Bitew, M. M., Gebremichael, M., Ghebremichael, L. T., and Bayissa, Y. A.: Evaluation of High-Resolution Satellite Rainfall Products through Streamflow Simulation in a Hydrological Modeling of a Small Mountainous Watershed in Ethiopia, Journal of Hydrometeorology, 13, 338-350, 10.1175/2011jhm1292.1, 2011.

Bouwer, L. M., Aerts, J. C. J. H., Van de Coterlet, G. M., Van de Giessen, N., Gieske, A., and Manaerts, C.: Evaluating downscaling methods for preparing Global Circulation Model

(GCM) data for hydrological impact modelling. Chapter 2, in Aerts, J.C.J.H. & Droogers, P.

Brown, A. M.: A new software for carrying out one-way ANOVA post hoc tests, Comput. Methods Programs Biomed., 79(1), 89–95, doi:https://doi.org/10.1016/j.cmpb.2005.02.007, 2005.

(Eds.), Climate Change in Contrasting River Basins: Adaptation Strategies for Water, Food and Environment. (pp. 25-47). Wallingford, UK: Cabi Press., 2004.

Cecinati, F., Rico-Ramirez, M. A., Heuvelink, G. B. M., and Han, D.: Representing radar rainfall uncertainty with ensembles based on a time-variant geostatistical error modelling approach, Journal of Hydrology, 548, 391-405, http://dx.doi.org/10.1016/j.jhydrol.2017.02.053, 2017.

Cohen Liechti, T., Matos, J. P., Boillat, J. L., and Schleiss, A. J.: Comparison and evaluation of satellite derived precipitation products for hydrological modeling of the Zambezi River Basin, Hydrol. Earth Syst. Sci., 16, 489-500, 2012.

Cuvelier, C., Thunis, P., Vautard, R., Amann, M., Bessagnet, B., Bedogni, M., Berkowicz, R., Brandt, J., Brocheton, F., Builtjes, P., Carnavale, C., Coppalle, A., Denby, B., Douros, J., Graf, A., Hellmuth, O., Hodzic, A., Honoré, C., Jonson, J., Kerschbaumer, A., de Leeuw, F., Minguzzi, E., Moussiopoulos, N., Pertot, C., Peuch, V. H., Pirovano, G., Rouil, L., Sauter, F., Schaap, M., Stern, R., Tarrason, L., Vignati, E., Volta, M., White, L., Wind, P., and Zuber, A.: CityDelta: A model intercomparison study to explore the impact of emission reductions in European cities in 2010, Atmospheric Environment, 41, 189-207, http://dx.doi.org/10.1016/j.atmosenv.2006.07.036, 2007.

Dennis, R., Fox, T., Fuentes, M., Gilliland, A., Hanna, S., Hogrefe, C., Irwin, J., Rao, S. T., Scheffe, R., Schere, K., Steyn, D., and Venkatram, A.: A framework for evaluating regional-scale numerical photochemical modeling systems, Environmental Fluid Mechanics, 10, 471-489, 10.1007/s10652-009-9163-2, 2010.

Dinku, T., Chidzambwa, S., Ceccato, P., Connor, S. J., and Ropelewski, C. F.: Validation of high-resolution satellite rainfall products over complex terrain, International Journal of Remote Sensing, 29, 4097-4110, 10.1080/01431160701772526, 2008.

Fang, G. H., Yang, J., Chen, Y. N., and Zammit, C.: Comparing bias correction methods in downscaling meteorological variables for a hydrologic impact study in an arid area in China, Hydrol. Earth Syst. Sci., 19, 2547-2559, 10.5194/hess-19-2547-2015, 2015.

Field , A.: Discovering statistics using SPSS 2nd ed. Sage Publications, 2009.

Fylstra, D., Lasdon, L., Watson, J., and Waren, A.: Design and Use of the Microsoft Excel Solver, Interfaces, 28, 29-55, doi:10.1287/inte.28.5.29, 1998.

Gao, Y. C., and Liu, M. F.: Evaluation of high-resolution satellite precipitation products using rain gauge observations over the Tibetan Plateau, Hydrol. Earth Syst. Sci., 17, 837-849, 10.5194/hess-17-837-2013, 2013.

Gebregiorgis, A. S., Tian, Y., Peters-Lidard, C. D., and Hossain, F.: Tracing hydrologic model simulation error as a function of satellite rainfall estimation bias components and land use and land cover conditions, Water Resources Research, 48, n/a-n/a, 10.1029/2011wr011643, 2012.

Grillakis, M. G., Koutroulis, A. G., Daliakopoulos, I. N., and Tsanis, I. K.: A method to preserve trends in quantile mapping bias correction of climate modeled temperature, Earth Syst. Dynam. Discuss., 2017, 1-26, 10.5194/esd-2017-53, 2017.

Gutjahr, O. and Heinemann, G.: Comparing precipitation bias correction methods for high-resolution regional climate simulations using COSMO-CLM, Theor. Appl. Climatol., 114(3–4), 511–529, doi:10.1007/s00704-013-0834-z, 2013.

Habib, E., ElSaadani, M., and Haile, A. T.: Climatology-Focused Evaluation of CMORPH and TMPA Satellite Rainfall Products over the Nile Basin, Journal of Applied Meteorology and Climatology, 51, 2105-2121, 10.1175/jamc-d-11-0252.1, 2012a.

Habib, E., Haile, A. T., Tian, Y., and Joyce, R. J.: Evaluation of the High-Resolution CMORPH Satellite Rainfall Product Using Dense Rain gauge Observations and Radar-Based Estimates, Journal of Hydrometeorology, 13, 1784-1798, 10.1175/jhm-d-12-017.1, 2012b.

Habib, E., Haile, A., Sazib, N., Zhang, Y., and Rientjes, T.: Effect of Bias Correction of Satellite-Rainfall Estimates on Runoff Simulations at the Source of the Upper Blue Nile, Remote Sensing, 6, 6688-6708, 2014.

Haile, A. T., Rientjes, T., Gieske, A., and Gebremichael, M.: Rainfall Variability over Mountainous and Adjacent Lake Areas: The Case of Lake Tana Basin at the Source of the Blue Nile River, Journal of Applied Meteorology and Climatology, 48, 1696-1717, 10.1175/2009JAMC2092.1, 2009.

Haile, A. T., Habib, E., and Rientjes, T. H. M.: Evaluation of the climate prediction center CPC morphing technique CMORPH rainfall product on hourly time scales over the source of the Blue Nile river, Hydrological processes, 27, 1829-1839, 2013.

Haile, A. T., Yan, F., and Habib, E.: Accuracy of the CMORPH satellite-rainfall product over Lake Tana Basin in Eastern Africa, Atmospheric Research. *In Press, Accepted manuscript*, http://dx.doi.org/10.1016/j.atmosres.2014.11.011, 2014.

Haile, A. T., Yan, F., and Habib, E.: Accuracy of the CMORPH satellite-rainfall product over Lake Tana Basin in Eastern Africa, Atmospheric Research, 163, 177-187, http://dx.doi.org/10.1016/j.atmosres.2014.11.011, 2015.

Heidinger, H., Yarlequé, C., Posadas, A., and Quiroz, R.: TRMM rainfall correction over the Andean Plateau using wavelet multi-resolution analysis, International Journal of Remote Sensing, 33, 4583-4602, 10.1080/01431161.2011.652315, 2012.

Hempel, S., Frieler, K., Warszawski, L., Schewe, J., and Piontek, F.: A trend-preserving bias correction - the ISI-MIP approach, Earth Syst. Dynam., 4, 219-236, 10.5194/esd-4-219-2013, 2013.

Hughes, D. A.: Comparison of satellite rainfall data with observations from gauging station networks, Journal of Hydrology, 327, 399-410, http://dx.doi.org/10.1016/j.jhydrol.2005.11.041, 2006.

Ines, A. V. M., and Hansen, J. W.: Bias correction of daily GCM rainfall for crop simulation studies, Agricultural and Forest Meteorology, 138, 44-53, http://dx.doi.org/10.1016/j.agrformet.2006.03.009, 2006.

Jiang, S.-h., Zhou, M., Ren, L.-l., Cheng, X.-r., and Zhang, P.-j.: Evaluation of latest TMPA and CMORPH satellite precipitation products over Yellow River Basin, Water Science and Engineering, 9, 87-96, http://dx.doi.org/10.1016/j.wse.2016.06.002, 2016.

Johnson, F. and Sharma, A.: Accounting for interannual variability: A comparison of options for water resources climate change impact assessments, Water Resour. Res., 47(4), doi:10.1029/2010WR009272, 2011.

Katiraie-Boroujerdy, P., Nasrollahi, N., Hsu, K., and Sorooshian, S.: Evaluation of satellite-based precipitation estimation over Iran, Elsevier, Kidlington, ROYAUME-UNI, 15 pp., 2013.

Khan, S. I., Hong, Y., Gourley, J. J., Khattak, M. U. K., Yong, B., and Vergara, H. J.: Evaluation of three high-resolution satellite precipitation estimates: Potential for monsoon monitoring over Pakistan, Advances in Space Research, 54, 670-684, http://dx.doi.org/10.1016/j.asr.2014.04.017, 2014.

Koutsouris, A. J., Chen, D., and Lyon, S. W.: Comparing global precipitation data sets in eastern Africa: a case study of Kilombero Valley, Tanzania, Int. J. Climatol., 36, 2000-2014, 10.1002/joc.4476, 2016.

Kucuk, U., Eyuboglu, M., Kucuk, H. O. and Degirmencioglu, G.: Importance of using proper post hoc test with ANOVA, Int. J. Cardiol., 209, 346, doi:10.1016/j.ijcard.2015.11.061, 2018.

Leander, R., Buishand, T. A., van den Hurk, B. J. J. M. and de Wit, M. J. M.: Estimated changes in flood quantiles of the river Meuse from resampling of regional climate model output, J. Hydrol., 351(3–4), 331–343, doi:10.1016/j.jhydrol.2007.12.020, 2008.

Lenderink, G., Buishand, A. and van Deursen, W.: Estimates of future discharges of the river Rhine using two scenario methodologies: direct versus delta approach, Hydrol. Earth Syst. Sci., 11(3), 1145–1159, doi:10.5194/hess-11-1145-2007, 2007.

Li, J., and Heap, A. D.: A review of comparative studies of spatial interpolation methods in environmental sciences: Performance and impact factors, Ecological Informatics, 6, 228-241, http://dx.doi.org/10.1016/j.ecoinf.2010.12.003, 2011.

Liu, J., Duan, Z., Jiang, J., and Zhu, A.-X.: Evaluation of Three Satellite Precipitation Products TRMM 3B42, CMORPH, and PERSIANN over a Subtropical Watershed in China, Advances in Meteorology, 2015, 13, 10.1155/2015/151239, 2015.

Liu, Z.: Comparison of precipitation estimates between Version 7 3-hourly TRMM Multi-Satellite Precipitation Analysis (TMPA) near-real-time and research products, Atmospheric Research, 153, 119-133, http://dx.doi.org/10.1016/j.atmosres.2014.07.032, 2015.

Lo Conti, F., Hsu, K.-L., Noto, L. V., and Sorooshian, S.: Evaluation and comparison of satellite precipitation estimates with reference to a local area in the Mediterranean Sea, Atmospheric Research, 138, 189-204, http://dx.doi.org/10.1016/j.atmosres.2013.11.011, 2014.

Maraun, D.: Bias Correcting Climate Change Simulations - a Critical Review, Current Climate Change Reports, 2, 211-220, 10.1007/s40641-016-0050-x, 2016.

Marcos, R., Llasat, M. C., Quintana-Seguí, P., and Turco, M.: Use of bias correction techniques to improve seasonal forecasts for reservoirs — A case-study in northwestern Mediterranean, Science of The Total Environment, 610–611, 64-74, https://doi.org/10.1016/j.scitotenv.2017.08.010, 2018.

Matos, J. P., Cohen Liechti, T., Juízo, D., Portela, M. M., and Schleiss, A. J.: Can satellite based pattern-oriented memory improve the interpolation of sparse historical rainfall records?, Journal of Hydrology, 492, 102-116, http://dx.doi.org/10.1016/j.jhydrol.2013.04.014, 2013.

Meier, P., Frömelt, A., and Kinzelbach, W.: Hydrological real-time modelling in the Zambezi river basin using satellite-based soil moisture and rainfall data., Hydrol. Earth Syst. Sci., 15, 999-1008, 2011.

Meyer, H., Drönner, J., and Nauss, T.: Satellite-based high-resolution mapping of rainfall over southern Africa, Atmos. Meas. Tech., 10, 2009-2019, 10.5194/amt-10-2009-2017, 2017.

Moazami, S., Golian, S., Kavianpour, M. R., and Hong, Y.: Comparison of PERSIANN and V7 TRMM Multi-satellite Precipitation Analysis (TMPA) products with rain gauge data over Iran, International Journal of Remote Sensing, 34, 8156-8171, 10.1080/01431161.2013.833360, 2013.

Müller, M. F., and Thompson, S. E.: Bias adjustment of satellite rainfall data through stochastic modeling: Methods development and application to Nepal, Advances in Water Resources, 60, 121-134, http://dx.doi.org/10.1016/j.advwatres.2013.08.004, 2013.

Najmaddin, P. M., Whelan, M. J., and Balzter, H.: Application of Satellite-Based Precipitation Estimates to Rainfall-Runoff Modelling in a Data-Scarce Semi-Arid Catchment, Climate, 5, 32, 2017.

NIST/SEMATECH: e-handbook of statistical methods. Croarkin, C., Tobias, P., and Zey, C. (Eds.), NIST ;, [Gaithersburg, Md.] :, 2001.

Pereira Filho, A. J., Carbone, R. E., Janowiak, J. E., Arkin, P., Joyce, R., Hallak, R., and Ramos, C. G. M.: Satellite Rainfall Estimates Over South America – Possible Applicability to the Water Management of Large Watersheds1, JAWRA Journal of the American Water Resources Association, 46, 344-360, 10.1111/j.1752-1688.2009.00406.x, 2010.

Rientjes, T., Haile, A. T., and Fenta, A. A.: Diurnal rainfall variability over the Upper Blue Nile Basin: A remote sensing based approach, International Journal of Applied Earth Observation and Geoinformation, 21, 311-325, http://dx.doi.org/10.1016/j.jag.2012.07.009, 2013a.

Rientjes, T. H. M., Muthuwatta, L. P., Bos, M. G., Booij, M. J., and Bhatti, H. A.: Multi-variable calibration of a semi-distributed hydrological model using streamflow data and satellite-based evapotranspiration, Journal of Hydrology, 505, 276-290, http://dx.doi.org/10.1016/j.jhydrol.2013.10.006, 2013b.

Romano, F., Cimini, D., Nilo, S., Di Paola, F., Ricciardelli, E., Ripepi, E., and Viggiano, M.: The Role of Emissivity in the Detection of Arctic Night Clouds, Remote Sensing, 9, 406, 2017.

Romilly, T. G., and Gebremichael, M.: Evaluation of satellite rainfall estimates over Ethiopian river basins, Hydrol. Earth Syst. Sci., 15, 1505-1514, 10.5194/hess-15-1505-2011, 2011.

Seo, D. J., Breidenbach, J. P., and Johnson, E. R.: Real-time estimation of mean field bias in radar rainfall data, Journal of Hydrology, 223, 131-147, http://dx.doi.org/10.1016/S0022-1694(99)00106-7, 1999.

Shrestha, M. S.: Bias-adjustment of satellite-based rainfall estimates over the central Himalayas of Nepal for flood prediction. PhD thesis, Kyoto University, 2011.

Smiatek, G., Kunstmann, H., and Senatore, A.: EURO-CORDEX regional climate model analysis for the Greater Alpine Region: Performance and expected future change, Journal of Geophysical Research: Atmospheres, 121, 7710-7728, 10.1002/2015JD024727, 2016.

Srivastava, P. K., Islam, T., Gupta, M., Petropoulos, G., and Dai, Q.: WRF Dynamical Downscaling and Bias Correction Schemes for NCEP Estimated Hydro-Meteorological Variables, Water Resources Management, 29, 2267-2284, 10.1007/s11269-015-0940-z, 2015.

Switanek, M. B., Troch, P. A., Castro, C. L., Leuprecht, A., Chang, H. I., Mukherjee, R., and Demaria, E. M. C.: Scaled distribution mapping: a bias correction method that preserves raw climate model projected changes, Hydrol. Earth Syst. Sci., 21, 2649-2666, 10.5194/hess-21-2649-2017, 2017.

Taylor, K. E.: Summarizing multiple aspects of model performance in a single diagram, Journal of Geophysical Research: Atmospheres, 106, 7183-7192, 10.1029/2000JD900719, 2001.

Tesfagiorgis, K., Mahani, S. E., Krakauer, N. Y., and Khanbilvardi, R.: Bias correction of satellite rainfall estimates using a radar-gauge product – a case study in Oklahoma (USA), Hydrol. Earth Syst. Sci., 15, 2631-2647, 10.5194/hess-15-2631-2011, 2011.

Themeßl, M. J., Gobiet, A., and Heinrich, G.: Empirical-statistical downscaling and error correction of regional climate models and its impact on the climate change signal, Clim. Change, 112, 449–468 2012.

Thiemig, V., Rojas, R., Zambrano-Bigiarini, M., Levizzani, V., and De Roo, A.: Validation of Satellite-Based Precipitation Products over Sparsely Gauged African River Basins, Journal of Hydrometeorology, 13, 1760-1783, 10.1175/jhm-d-12-032.1, 2012.

Thiemig, V., Rojas, R., Zambrano-Bigiarini, M., and De Roo, A.: Hydrological evaluation of satellite-based rainfall estimates over the Volta and Baro-Akobo Basin, Journal of Hydrology, 499, 324-338, 10.1016/j.jhydrol.2013.07.012, 2013.

Thorne, V., Coakeley, P., Grimes, D., and Dugdale, G.: Comparison of TAMSAT and CPC rainfall estimates with rain gauges, for southern Africa, International Journal of Remote Sensing, 22, 1951-1974, 10.1080/01431160118816, 2001.

Tian, Y., Peters-Lidard, C. D., and Eylander, J. B.: Real-Time Bias Reduction for Satellite-Based Precipitation Estimates, Journal of Hydrometeorology, 11, 1275-1285, 10.1175/2010JHM1246.1, 2010.

Tobin, K. J., and Bennett, M. E.: Adjusting Satellite Precipitation Data to Facilitate Hydrologic Modeling, Journal of Hydrometeorology, 11, 966-978, doi:10.1175/2010JHM1206.1, 2010.

Toté, C., Patricio, D., Boogaard, H., van der Wijngaart, R., Tarnavsky, E., and Funk, C.: Evaluation of Satellite Rainfall Estimates for Drought and Flood Monitoring in Mozambique, Remote Sensing, 7, 1758, 2015.

Tsidu, G. M.: High-Resolution Monthly Rainfall Database for Ethiopia: Homogenization, Reconstruction, and Gridding, Journal of Climate, 25, 8422-8443, 10.1175/JCLI-D-12-00027.1, 2012.

Tumbare, M. J.: Management of River Basins and Dams: The Zambezi River Basin, edited by: Tumbare, M. J., Taylor & Francis, 318 pp., 2000.

Tumbare, M. J.: The Management of the Zambezi River Basin and Kariba Dam, Bookworld Publishers, Lusaka, 2005.

Valdés-Pineda, R., Demaría, E. M. C., Valdés, J. B., Wi, S., and Serrat-Capdevilla, A.: Bias correction of daily satellite-based rainfall estimates for hydrologic forecasting in the Upper Zambezi, Africa, Hydrol. Earth Syst. Sci. Discuss., 2016, 1-28, 10.5194/hess-2016-473, 2016.

Vernimmen, R. R. E., Hooijer, A., Mamenun, Aldrian, E., and van Dijk, A. I. J. M.: Evaluation and bias correction of satellite rainfall data for drought monitoring in Indonesia, Hydrol. Earth Syst. Sci., 16, 133-146, 10.5194/hess-16-133-2012, 2012.

Wehbe, Y., Ghebreyesus, D., Temimi, M., Milewski, A., and Al Mandous, A.: Assessment of the consistency among global precipitation products over the United Arab Emirates, Journal of Hydrology: Regional Studies, 12, 122-135, http://dx.doi.org/10.1016/j.ejrh.2017.05.002, 2017.

Wilks, D.: Statistical Methods in the Atmospheric Sciences, 2nd ed., Academic Press, Burlington, Mass, 2006.

Woody, J., Lund, R., and Gebremichael, M.: Tuning Extreme NEXRAD and CMORPH Precipitation Estimates, Journal of Hydrometeorology, 15, 1070-1077, 10.1175/jhm-d-13-0146.1, 2014.

World Bank: The Zambezi River Basin : A Multi-Sector Investment Opportunities Analysis - Summary Report. World Bank. © World Bank. https://openknowledge.worldbank.org/handle/10986/2958 License: Creative Commons Attribution CC BY 3.0., 2010a.

World Bank: The Zambezi River Basin: A Multi-Sector Investment Opportunities Analysis, Volume 2 Basin Development Scenarios, 2010b.

Worqlul, A. W., Maathuis, B., Adem, A. A., Demissie, S. S., Langan, S., and Steenhuis, T. S.: Comparison of rainfall estimations by TRMM 3B42, MPEG and CFSR with ground-observed data for the Lake Tana basin in Ethiopia, Hydrol. Earth Syst. Sci., 18, 4871-4881, 10.5194/hess-18-4871-2014, 2014.

Wu, L., and Zhai, P.: Validation of daily precipitation from two high-resolution satellite precipitation datasets over the Tibetan Plateau and the regions to its east, Acta Meteorol Sin, 26, 735-745, 10.1007/s13351-012-0605-2, 2012.

Yang, X., Xie, X., Liu, D. L., Ji, F., and Wang, L.: Spatial Interpolation of Daily Rainfall Data for Local Climate Impact Assessment over Greater Sydney Region, Advances in Meteorology, 2015, 12, 10.1155/2015/563629, 2015.

Yin, Z. Y., Zhang, X., Liu, X., Colella, M., and Chen, X.: An assessment of the biases of satellite rainfall estimates over the tibetan plateau and correction methods based on topographic analysis, Journal of Hydrometeorology, 9, 301, 2008.

Yoo, C., Park, C., Yoon, J., and Kim, J.: Interpretation of mean-field bias correction of radar rain rate using the concept of linear regression, Hydrological Processes, 28, 5081-5092, 10.1002/hyp.9972, 2014.

Zulkafli, Z., Buytaert, W., Onof, C., Manz, B., Tarnavsky, E., Lavado, W., and Guyot, J.-L.: A Comparative Performance Analysis of TRMM 3B42 (TMPA) Versions 6 and 7 for Hydrological Applications over Andean–Amazon River Basins, Journal of Hydrometeorology, 15, 581-592, doi:10.1175/JHM-D-13-094.1, 2014.

Appendix 1: Rain gauge stations in the Zambezi sub-basins showing x and y location, sub-basin they belong to, year of data availability, % of missing gaps, station elevation and distance from large-scale water bodies.

Station	Sub-basin	Zambezi classification	X Coord	Y Coord	Start date	End Date	% gaps (missing records)	Elevation (m)	Distance from lake (km)	MAP Gauge (mm/yr)	MAP CMORPH (mm/yr)
Marromeu	Zambezi Delta	Lower Zambezi	36.95	-18.28	29/05/2007	31/12/2013	0.37	3	90	1075	1080
Caia	Zambezi Delta	Lower Zambezi	35.38	-17.82	29/05/2007	31/12/2013	0.13	28	265	970.5	975
Nsanje	Shire	Lower Zambezi	35.27	-16.95	01/01/1998	31/12/2013	3.49	39	157	906.4	874
Makhanga	Shire	Lower Zambezi	35.15	-16.52	01/01/1998	31/12/2013	9.43	48	113	778.3	771
Nchalo	Shire	Lower Zambezi	34.93	-16.23	01/01/1998	31/12/2013	0.60	64	96	726.3	725
Ngabu	Shire	Lower Zambezi	34.95	-16.50	01/01/1998	3112/2010	0.74	89	123	736	752
Chikwawa	Shire	Lower Zambezi	34.78	-16.03	01/01/1998	31/12/2010	0.93	107	77	731.3	725
Tete (Chingodzi)	Tete	Lower Zambezi	33.58	-16.18	29/05/2007	31/12/2013	0.17	151	135	684.3	677
Chingodzi	Shire	Lower Zambezi	34.63	-16.00	29/05/2007	10/01/2013	11.8	280	101	737.7	735
Zumbo	Shire	Lower Zambezi	30.45	-15.62	29/05/2007	12/09/2012	0.16	345	<5	859.3	862
Mushumbi	Kariba	Middle Zambezi	30.56	-16.15	11/06/2008	11/12/2013	7.47	369	43	852.2	1028
Kanyemba	Tete	Middle Zambezi	30.42	-15.63	01/01/1998	30/03/2013	5.86	372	<5	859.3	862
Morrumbala	Zambezi Delta	Lower Zambezi	35.58	-17.35	29/05/2007	10/01/2013	13.3	378	206	1011.7	1002

Mágoè	Tete	Middle Zambezi	31.75	-15.82	01/01/2009	31/12/2013	9.6	427	10	821.7	646
Muzarabani	Tete	Middle Zambezi	31.01	-16.39	01/01/1998	31/12/2013	1.14	430	49	821.3	887
Monkey	Shire	Lower Zambezi	34.92	-14.08	01/01/1998	30/11/2010	0.00	478	<5	988.5	1012
Mangochi	Shire	Lower Zambezi	35.25	-14.47	01/01/1998	31/12/2010	0.02	481	<5	1015	1042
Rukomechi	Kariba	Middle Zambezi	29.38	-16.13	01/01/1998	31/12/2013	6.40	530	68	803.9	800
Mutarara	Shire	Lower Zambezi	33.00	-17.38	29/05/2007	10/01/2013	11.7	548	201	888.2	859
Mfuwe	Luangwa	Middle Zambezi	31.93	-13.27	01/01/1998	31/12/2010	2.70	567	246	1092.5	1112
Mimosa	Shire	Lower Zambezi	35.62	-16.07	01/01/1998	31/12/2010	3.96	616	72	964.4	962
Kariba	Kariba	Middle Zambezi	28.80	-16.52	01/01/1998	31/12/2013	0.01	618	21	980.6	767
Balaka	Shire	Lower Zambezi	34.97	-14.98	01/01/1998	30/04/2010	0.78	618	24	778.2	754
Thyolo	Shire	Lower Zambezi	35.13	-16.13	01/01/1998	31/12/2010	0.11	624	86	789.6	787
Chileka	Shire	Lower Zambezi	34.97	-15.67	01/01/1998	31/12/2013	0.60	744	64	720.7	708
Fingoe	Tete	Middle Zambezi	31.88	-15.17	01/01/2009	31/12/2013	5.9	881	44	859.4	867
Muze	Tete	Zambezi	31.38	-14.95	01/01/2009	31/12/2013	8.8	888	75	879	800
Neno	Shire	Lower Zambezi	34.65	-15.40	01/01/1998	01/01/2010	9.14	903	64	810.7	813
Zámbue	Tete	Middle Zambezi	30.80	-15.11	01/01/2009	31/12/2013	9.8	950	56	870.5	1006
Mt Darwin	Tete	Middle Zambezi	31.58	-16.78	01/01/1998	02/03/2008	5.00	962	94	832.3	839
Chipata	Shire	Lower Zambezi	32.58	-13.55	01/01/1998	13/08/2003	1.11	995	179	1009.4	1028
Makoka	Shire	Lower Zambezi	35.18	-15.53	01/01/1998	31/12/2010	0.00	996	27	716.9	685
Livingstone	Kariba	Middle Zambezi	25.82	-17.82	01/01/1998	31/12/2013	0.00	996	107	761.2	765
Senanga	Barotse	Upper Zambezi	23.27	-16.10	01/01/1998	31/12/2013	8.90	1001	444	856.1	860
Petauke	Luangwa	Middle Zambezi	31.28	-14.25	01/02/1998	31/12/2013	0.40	1006	155	936.9	912

Msekera	Luangwa	Middle Zambezi	32.57	-13.65	01/03/1998	31/12/2015	19.7	1028	179	1009.4	1028
Kalabo	Lungue Bungo	Upper Zambezi	22.70	-14.85	01/01/1998	31/12/2011	5.20	1033	582	835.8	838
Mongu	Barotse	Upper Zambezi	23.15	-15.25	01/01/1998	31/12/2013	0.51	1052	518	847.9	843
Kasungu	Shire	Lower Zambezi	33.47	-13.02	01/01/2003	31/07/2013	0.00	1063	89	793.2	783
Victoria Falls	Kariba	Middle Zambezi	25.85	-18.10	01/01/1998	31/12/2013	2.26	1065	107	740.8	742
Bolero	Luangwa	Middle Zambezi	33.78	-11.02	01/01/2003	31/05/2013	0.00	1070	38	639	577
Pandamatenga	Kariba	Middle Zambezi	25.63	-18.53	01/01/1998	31/12/2013	0.01	1071	151	709	771
Zambezi	Lungue Bungo	Upper Zambezi	23.12	-13.53	01/01/1998	31/12/2013	1.60	1075	611	982	976
Kabompo	Kabombo	Upper Zambezi	24.20	-13.60	01/01/1998	30/04/2005	0.08	1086	505	1045.9	1055
Chichiri	Shire	Lower Zambezi	35.05	-15.78	01/01/1998	31/12/2010	0.00	1136	40	717.3	744
Chitedze	Shire	Lower Zambezi	33.63	-13.97	01/01/2003	30/04/2013	0.00	1150	84	808.5	806
Lundazi	Luangwa	Middle Zambezi	33.20	-12.28	01/01/2003	30/04/2013	1.40	1151	91	778.8	774
Guruve	Tete	Middle Zambezi	30.70	-16.65	01/01/1998	30/03/2013	0.02	1159	86	866.1	870
Kaoma	Barotse	Upper Zambezi	24.80	-14.80	01/01/1998	31/11/2013	9.89	1162	358	950	956
Bvumbwe	Shire	Lower Zambezi	35.07	-15.92	01/01/1998	01/01/2011	0.00	1172	59	762.2	744
Kasempa	Kafue	Middle Zambezi	25.85	-13.53	01/01/1998	31/12/2013	9.10	1185	431	1029.4	1022
Kabwe	Luangwa	Middle Zambezi	28.47	-14.45	01/01/1998	13/10/2012	1.54	1209	230	960.6	956
Chitipa	Shire	Lower Zambezi	33.27	-9.70	01/01/2003	06/01/2013	0.05	1288	62	1133.5	1156
Mwinilunga	Kabompo	Upper Zambezi	24.43	-11.75	01/01/1998	31/12/2013	4.81	1319	520	1001.3	997
Karoi	Tete	Middle Zambezi	29.62	-16.83	01/01/1998	31/12/2004	15.08	1345	88	825.8	819
Solwezi	Kafue	Middle Zambezi	26.38	-12.18	01/01/1998	31/12/2013	0.02	1372	356	1105.2	1105
Harare (Belvedere)	Tete	Middle Zambezi	31.02	-17.83	01/01/1998	31/03/2013	7.80	1472	209	901.4	902

Harare(Kutsaga)	Tete	Middle Zambezi	31.13	-17.92	01/01/2004	30/09/2010	0.55	1488	209	901.4	902
Mvurwi	Tete	Middle Zambezi	30.85	-17.03	01/01/1998	11/12/2000	0.00	1494	102	834.2	828
Dedza	Shire	Lower Zambezi	34.25	-14.32	01/01/2003	31/10/2012	0.00	1575	44	762.8	762

Appendix 2: Bias correction scheme based Taylor Diagram performance indicators (correlation coefficients, standard deviations and RMSE) of rain gauge (reference) vs CMORPH estimations (corrected and uncorrected), period 1998-2013, for Lower, Middle and Upper Zambezi Basin.

Sub-basin	Rainfall estimate	RMSE (mm/day)	Correlation Coefficient	Standard Deviation (mm/day)
Lower Zambezi	Gauge			9.38
	R-CMORPH	9.98	0.46	8.00
	PT	10.41	0.57	8.52
	QME	9.15	0.55	6.98
	EZ	10.48	0.62	6.35
	DT	9.30	0.56	6.55
	STB	8.59	0.72	7.17
Middle Zambezi	Gauge			7.94
	R-CMORPH	8.12	0.49	7.44
	PT	7.87	0.62	6.84
	QME	7.51	0.60	6.00
	EZ	10.69	0.65	6.93
	DT	8.04	0.59	6.96
	STB	7.49	0.76	6.81
Upper Zambezi	Gauge			8.29
	R-CMORPH	7.23	0.45	6.60
	PT	7.97	0.62	7.29
	QME	8.05	0.55	7.12
	EZ	11.50	0.60	8.13
	DT	7.85	0.55	6.45
	STB	0.54	0.74	7.29